

REPORT DOCUMENTATION PAGE		READ INSTRUCTIONS BEFORE COMPLETING FORM
1. REPORT NUMBER NRL Report 7809	2. GOVT ACCESSION NO.	3. RECIPIENT'S CATALOG NUMBER
4. TITLE (and Subtitle) EFFECTS OF A FLUCTUATING TEMPERATURE FIELD ON THE SPATIAL COHERENCE OF ACOUSTIC SIGNALS		5. TYPE OF REPORT & PERIOD COVERED Interim report on a continuing NRL Problem.
		6. PERFORMING ORG. REPORT NUMBER
7. AUTHOR(s) M. J. Beran, J. J. McCoy, and B. B. Adams		8. CONTRACT OR GRANT NUMBER(s)
9. PERFORMING ORGANIZATION NAME AND ADDRESS Naval Research Laboratory Washington, D.C. 20375		10. PROGRAM ELEMENT, PROJECT, TASK AREA & WORK UNIT NUMBERS NRL Problem S01-55 XF52-552-700
11. CONTROLLING OFFICE NAME AND ADDRESS Department of the Navy Naval Electronics Systems Command Washington, D.C. 20360		12. REPORT DATE May 22, 1975
		13. NUMBER OF PAGES 48
14. MONITORING AGENCY NAME & ADDRESS (if different from Controlling Office)		15. SECURITY CLASS. (of this report) Unclassified
		15a. DECLASSIFICATION/DOWNGRADING SCHEDULE
16. DISTRIBUTION STATEMENT (of this Report) Approved for public release; distribution unlimited.		
17. DISTRIBUTION STATEMENT (of the abstract entered in Block 20, if different from Report)		
18. SUPPLEMENTARY NOTES		
19. KEY WORDS (Continue on reverse side if necessary and identify by block number) Acoustics Fluctuations, effects of Scattering (of sound waves) Sound propagation Wave propagation		
20. ABSTRACT (Continue on reverse side if necessary and identify by block number) A theoretical model has been developed for predicting the loss of spatial coherence of moderately low frequency acoustic signals (50 to 300 Hz) that results from the presence of a fluctuating temperature field caused by internal waves and by ocean turbulence. The model has been used to estimate limitations on the maximum useful length of a horizontal, linear, phased array the performance of which is degraded by the presence of the fluctuating temperature field. With the use of reported environmental data, this maximum length can be estimated by a simple algebraic formula: $L_x = 1.1(AA) L \exp(-3/2)(R) \exp(-2/3)$		

20. Abstract (Continued)

where L_x and R are measures of optimum array size and range, respectively, expressed in units of acoustic wave number ($2\pi/\text{wavelength}$) and $(AA) L$ is a combination of environmental terms. The parameter A squared, (AA) , is a measure of the strength of the horizontal spatial sound speed fluctuations and L is the average vertical correlation length; both of which are a result of the temperature microstructure.

Questions of the limits of both the theoretical model and of knowledge of some aspects of oceanic environmental conditions have been raised. Recommendations have been made for a series of future studies.

CONTENTS

INTRODUCTION	1
LOSS OF SPATIAL COHERENCE DUE TO SCATTERING BY THE TEMPERATURE MICROSTRUCTURE	4
CONCLUSIONS AND RECOMMENDATIONS	13
APPENDIX A — Single Scatter Solution	15
APPENDIX B — Multiple Scatter Solution	22
APPENDIX C — A Numerical Study	30
APPENDIX D — Effects of Nonhomogeneity, Reflection, and Source Size	37
APPENDIX E — Background Discussion of Aperture Problem	43

EFFECTS OF A FLUCTUATING TEMPERATURE FIELD ON THE SPATIAL COHERENCE OF ACOUSTIC SIGNALS

INTRODUCTION

A careful examination of sound-speed measurements taken at sea reveals the presence of weak fluctuations about an averaged, or mean, sound-speed profile. Because the cause of these fluctuations rests in variations in the temperature field, it has been commonly accepted to refer to the fluctuations as the thermal or temperature microstructure. Inasmuch as the length scales on which the fluctuations are measured range through thousands of meters, this appellation is something of a misnomer. However, we will retain the accepted terminology in this report.

An acoustic signal that propagates through the ocean will interact with the temperature microstructure, resulting in a scattered field that is characterized by irregular spatial and temporal variations. Although the local scattering is expected to be weak, by virtue of the weakness of the sound-speed fluctuations, the effects of this scattering are cumulative. Thus, the presence of the temperature microstructure results in an ultimate limitation on the detection capability of long-range sonar surveillance systems. In this report we investigate the question of range limitation as a consequence of the loss of spatial coherence of an incident signal that is scattered by the temperature microstructure. This loss of spatial coherence results in an upper limit on the useful size of a receiving array. Arrays of sizes larger than this useful limit will contain elements that will receive signals that are uncorrelated with one another, at the limiting pair separation distances, thereby precluding the possibility of coherently summing these signals to increase signal gain or to determine more accurately their direction of propagation.

At short ranges one can, by virtue of the weakness of the sound-speed fluctuations, obtain estimates of any desired statistic of the scattered signal by making use of a single scatter theory. Although the single scatter theory cannot be validly applied in the situation of interest to us, long-range propagation, it is still of indirect use because it can predict the local nature of the scattering phenomenon. Thus, for example, the single scatter solution illustrates that a characteristic of the ocean temperature microstructure of great importance as to its effects on acoustic signals is its strong anisotropy. This anisotropy is such that measured correlation lengths of fluctuating sound-speed records obtained from horizontal tow runs are orders of magnitude greater than any estimate of the largest correlation length for vertical lengths. It is not surprising, therefore, to find that the angular distribution of the locally scattered radiation field is anisotropic, with a much greater angular spread measured in a vertical plane than that measured in a horizontal plane. This conclusion leads to the further conclusion that the loss of spatial coherence with range will be much faster for receivers separated along a vertical line than it will for receivers separated along a horizontal line.

The dependence of the angular distribution of the locally scattered field on the signal wavelengths relative to sound-speed correlation lengths is considered in detail in Appendix A. The major conclusions for our studies are for the cases in which

$$\ell_{VM} \lesssim \bar{\lambda} \ll \ell_{Hm}$$

where $\bar{\lambda}$ is a characteristic signal wavelength, ℓ_{VM} is the maximum vertical sound-speed correlation length, and ℓ_{Hm} is the minimum horizontal sound-speed correlation length. For a signal incident in a horizontal direction it is shown that the locally scattered radiation field is confined to horizontal angles of the order of $\bar{\lambda}/2\pi\ell_{Hm}$ and vertical angles of the order of $(\bar{\lambda}/2\pi\ell_{Hm})^{1/2}$. Thus, we see that the angular spread in the horizontal plane is indeed much smaller than that in the vertical plane. However, we note the additional result that, although vertical scattering covers a wider angle than does horizontal scattering, it is still essentially a forward scattering. The vertical scattering is controlled by the ratio $\bar{\lambda}/2\pi\ell_{Hm}$ and not $\bar{\lambda}/2\pi\ell_{VM}$, as one might intuitively expect. This result is important because it indicates that a considerably larger amount of acoustic energy will reach the receiving array than would be the case should the vertical scattering be isotropic, as one might suspect from comparing the sizes of $\bar{\lambda}$ and ℓ_{VM} . Parenthetically, we might remark that the assumption that the local scattering is forward directed is crucial to the subsequent development of the theory that is the basis of this report.

Obtaining quantitative estimates of the loss of signal coherence over long propagation distances requires the identification of a suitable measure of coherence and the development of a theory capable of making predictions of this measure in the multiple scatter region. The measure of spatial coherence in terms of which our theory is formulated is the mutual coherence function, defined for narrowband signals by

$$\left\{ \hat{\Gamma}(\mathbf{x}_1, \mathbf{x}_2, \bar{\nu}) \right\} = \left\{ \hat{p}(\mathbf{x}_1, \bar{\nu}) \hat{p}^*(\mathbf{x}_2, \bar{\nu}) \right\} . \quad (1)$$

where \mathbf{x}_1 and \mathbf{x}_2 are the two positions of interest and $\bar{\nu}$ is the central frequency of the narrowband signal. The quantity $\hat{p}(\mathbf{x})$ is the complex acoustic pressure at position \mathbf{x} . The braces $\{ \}$ indicate an ensemble average; the asterisk indicates complex conjugation. Our reasons for the choice of this measure of coherence are threefold: (a) for the signal detection problem it is a recognized function appearing throughout the literature; (b) for the resolution problem it is, along with its Fourier transform, a most suitable measure of a coherence; (c) it is only in terms of this measure that valid multiple scatter solutions have been obtained.

For an infinite, coherent plane wave incident at the vertical plane, $z = 0$ (see Fig. 1); we have

$$\left\{ \hat{\Gamma}(\mathbf{x}_{1T}, \mathbf{x}_{2T}, 0; \bar{\nu}) \right\} = \hat{I}$$

where \mathbf{x}_{1T} and \mathbf{x}_{2T} denote position vectors locating two points in the $z = 0$ plane and \hat{I} is the intensity of the plane wave signal. In the case of a statistically homogeneous sound field $\left\{ \hat{\Gamma}(\mathbf{x}_{1T}, \mathbf{x}_{2T}, \bar{\nu}) \right\}$ measured at two points in the same vertical plane,

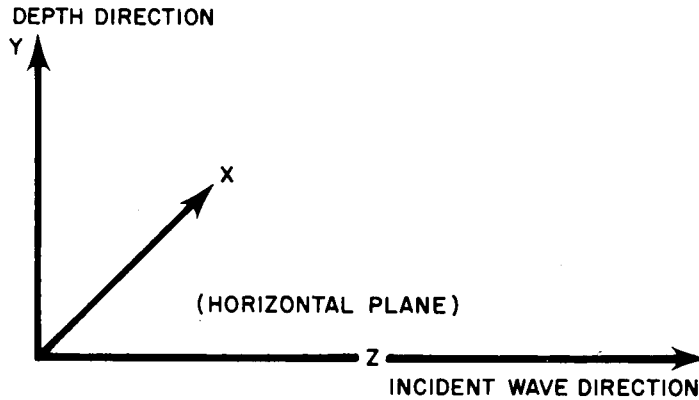


Fig. 1 — Problem geometry and choice of coordinate axes

perpendicular to the incident wave direction and located a distance z into the medium, is a function of transverse coordinate differences alone, provided z is large compared to the maximum horizontal correlation length: that is,

$$\{ \hat{\Gamma}(\mathbf{x}_1, \mathbf{x}_2; \bar{v}) \} = \{ \hat{\Gamma}(\mathbf{s}, z; \bar{v}) \}$$

where $\mathbf{s} = \mathbf{x}_{1T} - \mathbf{x}_{2T}$, provided $z \gg \ell_{HM}$. The value of $\{ \hat{\Gamma}(\mathbf{s}, z; \bar{v}) \}$ falls off, from a maximum value of \hat{I} at $\mathbf{s} = 0$, with increasing $|\mathbf{s}|$. A signal coherence length is defined by the condition that $\{ \hat{\Gamma}(\mathbf{s}, z; \bar{v}) \}$ be less than some prescribed percentage of \hat{I} for all $|\mathbf{s}|$ greater than this length. (We note that the coherence length defined in this way depends on the direction of \mathbf{s} .) Signals received by hydrophones separated by a distance that is greater than this coherence length are said to be uncorrelated. The coherent summing of such signals to increase the signal-to-noise ratio is, therefore, to no avail. Thus, the coherence length so defined is, in fact, an estimate of the maximum useful length for increasing the signal gain of a line array.

Furthermore, the two-dimensional Fourier transform of $\{ \hat{\Gamma}(\mathbf{s}, z; \bar{v}) \}$, denoted by $\{ \tilde{\Gamma}(\mathbf{k}_T, z; \bar{v}) \}$, where \mathbf{k}_T is the transverse wave number, gives the plane wave angular spectrum of the acoustic signal crossing the plane. The principal effect of the scattering by the temperature microstructure is to smear out the spatial delta-function dependence of the incident plane wave spectrum. This smearing represents an uncertainty in the direction of the incident plane wave signal and is the cause of the resolution limitation due to the scattering. The resolution limitation leads to a maximum useful array size because it is to no avail to construct arrays that are large enough to resolve angles smaller than the uncertainty that results from the scattering. (Larger arrays could prove useful for surveillance systems that use additional signal processing.) It is not difficult to show that the size limitation defined by the signal-detection problem is of the same order of magnitude as the size limitation defined by the resolution problem.

The signal coherence with the separation distance measured along a line that coincides with the original propagation direction is expected to be much greater than that measured along lines orthogonal to this direction. Although one might not expect to improve the resolution problem by using arrays that are aligned in this direction, it does appear that greater signal gains might be achieved.

In the next section, we discuss in detail the dependence of $\{\hat{\Gamma}(s, z; \bar{\nu})\}$ on the ocean temperature microstructure. Emphasis in this report is placed on separation distances measured along a horizontal line, consistent with the expected principal applications. An extremely simple expression, Eq. (17), that gives $\{\hat{\Gamma}(x_{12}, 0, z; \bar{\nu})\}$ in terms of signal frequency, range, and a single microstructure parameter, is obtained. Here, x_{12} is the horizontal separation distance. The development of the theory required for this discussion is given in Appendix B.

A summary, conclusions, and recommendations are given in the concluding section.

The report contains five appendixes. Appendixes A and B have already been mentioned. Appendix C presents the results of a numerical study in which the acoustic model was applied to some typical sea conditions. Appendix D is devoted to a discussion of the effects of a finite beam width, an inhomogeneous mean sound speed, and inhomogeneous statistics for the sound-speed fluctuations. Appendix E contains a brief discussion of prior work on the problem of interest.

LOSS OF SPATIAL COHERENCE DUE TO SCATTERING BY THE TEMPERATURE MICROSTRUCTURE

In this section we discuss the loss of spatial coherence of an original plane wave signal due to scattering by the temperature microstructure. The measure of spatial coherence chosen for our analysis is the mutual coherence function defined, for a time harmonic signal, by

$$\{\hat{\Gamma}(\mathbf{x}_1, \mathbf{x}_2, \bar{\nu})\} = \{\hat{p}^*(\mathbf{x}_1, \bar{\nu}) \hat{p}(\mathbf{x}_2, \bar{\nu})\} \quad (1)$$

where \mathbf{x}_1 , and \mathbf{x}_2 are the two positions of interest, $\bar{\nu}$ is the central frequency of the narrowband signal, and $\hat{p}(\mathbf{x}, \bar{\nu})$ is the complex pressure field at position \mathbf{x} . The original direction of the plane wave is restricted to lie in a horizontal plane. The coordinate axes used in presenting our results are illustrated in Fig. 1. The z axis lies along the original propagation direction; the x axis is orthogonal to the z axis and lies in a horizontal plane; and the y axis is orthogonal to the x and z axes, i.e., it is in the vertical, or depth, direction. The requisite theory for discussing the mutual coherence function for pairs of points located in a plane orthogonal to the original plane wave direction is developed in Appendix B. This theory is suitable for estimating the expected performance of either line arrays, or of billboard arrays.

We present the following results of the theoretical development in Appendix B to serve as the starting point for our discussion. For two points separated along the horizontal, or x axis, we have

$$\left\{ \hat{\Gamma}(x_{12}, 0, z) \right\} = \hat{I} \exp \left(- \left[\bar{\sigma}_2(0, 0) - \bar{\sigma}_2(x_{12}, 0) \right] z \right), \quad (2)$$

whereas for two points separated along the vertical, or y axis, we have

$$\left\{ \hat{\Gamma}(0, y_{12}, z) \right\} = \left(\hat{I} \frac{\bar{\sigma}_2(0, y_{12})}{\bar{\sigma}_2(0, 0)} + \left[1 - \frac{\bar{\sigma}_2(0, y_{12})}{\bar{\sigma}_2(0, 0)} \right] \exp \left[- \bar{\sigma}_2(0, 0) z \right] \right). \quad (3)$$

We have suppressed the \bar{v} . The separation distance between pairs of points are denoted by x_{12} (horizontal separation) and y_{12} (vertical separation); the original plane wave intensity is indicated by \hat{I} ; and, z denotes the range, or horizontal propagation distance. The temperature microstructure is described by the function $\bar{\sigma}_2(x_{12}, y_{12})$, which is given in terms of the correlation function associated with the sound speed fluctuations i.e. $\bar{\sigma}(x_{12}, s_y, s_z)$ according to

$$\bar{\sigma}_2(x_{12}, y_{12}) = \left(\frac{2}{\pi} \right)^{1/2} \frac{\bar{k}^3}{4} \int_0^\infty \frac{\cos \left(\frac{\bar{k} y_{12}^2}{2 s_z} - \frac{\pi}{4} \right)}{(k s_z)^{1/2}} \left(\int_{-\infty}^\infty \sigma(x_{12}, s_y, s_z) ds_y \right) ds_z. \quad (4)$$

Here, $\bar{k} = 2\pi/\bar{\lambda}$ denotes the wave number of the acoustic signal. The theory assumes a microstructure that is statistically homogeneous and does not include a mean sound profile or any boundary. These, and other factors not explicitly incorporated in the theory, are discussed in Appendix D. A detailed discussion of the approximations incorporated in the theory is given in Appendix B.

Both Eqs. (2) and (3) lead to the conclusion that the mutual coherence function reduces to \hat{I} for zero separation distance. As noted in the introduction, and discussed in detail in Appendix A, the local scattering by the temperature microstructure is essentially a forward scattering. This fact, and energy conservation requirements, necessitate that $\left\{ \hat{\Gamma}(0, 0, z) \right\} = \hat{I}$ for all ranges. Further, noting that $\bar{\sigma}_2(x_{12}, y_{12})$ approaches zero for large enough separation distances for all physically realistic temperature microstructures, we see that Eqs. (2) and (3) reduce to

$$\left\{ \hat{\Gamma}(x_{12}, 0, z) \right\} \approx \left\{ \hat{\Gamma}(0, y_{12}, z) \right\} \approx \hat{I} \exp \left[- \bar{\sigma}_2(0, 0) z \right], \quad (5)$$

provided that the separation distance s is large enough. The form of the r.h.s. of this equation is that of the mutual coherence function of a plane wave signal with intensity equal to $\hat{I} \exp[-\bar{\sigma}_2(0,0)z]$. This form suggests our interpreting the r.h.s. of Eq. (5) in terms of the relative amount of energy remaining in the completely coherent plane wave signal. Thus, $1/\bar{\sigma}_2(0,0)$ may be interpreted as a decay length; i.e., it gives a measure of the range at which a significant amount of energy has been scattered from the completely coherent initial signal into the partially coherent fluctuating signal. It, therefore, provides a measure of the limit of validity of the results based on a single scatter theory.

The degree of coherence of the fluctuating signal and its dependence on separation distance is seen to differ for separation distances measured along a horizontal line (the x axis) compared to distances measured along a vertical line (the y axis). This anisotropy is to be expected because the statistics of the sound-speed fluctuations causing the

scattering are likewise anisotropic. Careful consideration of Eqs. (2) through (4) allows the conclusion that the loss of coherence with separation distance, at a given range, is much greater for distances measured in the vertical direction than it is for distances measured in the horizontal direction. This result is in agreement with the conclusion, based on a single scatter calculation, that the angular distribution of the locally scattered field is broader in a vertical plane than it is in a horizontal plane.

In the subsequent discussion, we limit our attention to the loss of spatial coherence for points separated along the x axis. It is this loss that will determine the limitations in the ability to resolve the azimuth of the original signal. It is also this loss that will determine the limit of the ability to detect the presence of the signal in a noise field by coherently summing the signals received by the elements of a horizontal line array positioned normal to the incoming signal direction. A similar discussion, concentrating on points separated along the y axis, is possible. Order of magnitude estimates based on Eq. (3), however, indicate that the falloff of spatial coherence with vertical separation distance is great, so that for the ranges and signal frequencies of interest in our studies, considerably less signal gain may be achieved by vertical extension of an array.* For this first report we turn to Eq. (2), which indicates that the relevant quantity for our study is

$$\bar{\sigma}_2(0, 0) - \bar{\sigma}_2(x_{12}, 0) = \frac{\bar{k}^3}{4\pi^{1/2}} \int_0^\infty \frac{1}{(\bar{k} s_z)^{1/2}} \left(\int_{-\infty}^\infty [\sigma(0, s_y, s_z) - \sigma(x_{12}, s_y, s_z)] ds_y \right) ds_z \quad (6)$$

Since the experimental data required to make detailed predictions of index-of-refraction fluctuations with depth are largely lacking (almost all reported data are based on horizontal measurements, giving information only for $\sigma(x_{12}, 0, s_z)$), it is fortunate that our acoustic model does not require this detailed information but only requires the integral of $\sigma(x_{12}, s_y, s_z)$ over the depth coordinate. Although a simple relation need not exist between this integral and $\sigma(x_{12}, 0, s_z)$, we shall assume that one does,** and, in particular, assume that

$$\int_{-\infty}^\infty \sigma(x_{12}, s_y, s_z) ds_y = \ell_{yM} \sigma(x_{12}, 0, s_z) \quad (7)$$

where ℓ_{yM} is a weighted-average correlation length for measurements taken in the depth direction. In addition, we shall assume that the statistics of the microstructure are isotropic for measurements taken in a horizontal plane; i.e.,

$$\sigma(x_{12}, 0, s_z) = \sigma\sqrt{x_{12}^2 + s_z^2}, 0). \quad (8)$$

Introducing Eqs. (7) and (8) into Eq. (6) gives

* Noise rejection as contrasted with path resolution may call for exploitation of available vertical coherence to increase signal to noise gain.
 **For example, a sufficient condition for Eq. (27) is the independence of the fields in the vertical and horizontal directions.

$$\sigma_2(0, 0) - \bar{\sigma}_2(x_{12}, 0) = \frac{\bar{k}^3 \ell_{yM}}{8\pi^{1/2}} \int_{-\infty}^{\infty} \frac{\sigma(s_z, 0) - \sigma(\sqrt{s_z^2 + x_{12}^2}, 0) ds_z}{(\bar{k}s_z)^{1/2}} \quad (9)$$

Although the loss of spatial coherence can be discussed with the use of this expression, it proves convenient to discuss sound-speed fluctuations in terms of the one-dimensional spectrum; i.e., in terms of $\Phi_1(p)$, given by

$$\Phi_1(p) = \frac{1}{2\pi} \int_{-\infty}^{\infty} \sigma(q, 0) \exp(ipq) dq \quad (10)$$

where

$$q = \sqrt{x_{12}^2 + s_z^2} \quad (11)$$

The spectral function $\Phi_1(p)$ has the intuitively satisfying significance of subdividing the power of the fluctuations field into characteristic size intervals; eddy sizes, in the turbulence terminology.

By introducing the inverse of Eq. (10) into Eq. (9) and assuming that the orders of integration in the resulting expression can be interchanged, we can carry out the integration over s_z . The result is written

$$\bar{\sigma}_2(0, 0) - \bar{\sigma}_2(x_{12}, 0) = \frac{\bar{k}^{-5/2} \ell_{yM} x_{12}^{1/2}}{2^{3/2}} \int_0^{\infty} F(px_{12}) \Phi_1(p) dp \quad (12)$$

where

$$F(px_{12}) = \frac{1}{(px_{12})^{1/2}} - \frac{\Gamma\left(\frac{1}{4}\right)}{2^{3/2}} (px_{12})^{1/4} J_{-3/4}(px_{12}). \quad (13)$$

Here, $\Gamma(1/4)$ is a Gamma function and $J_{-3/4}$ is a Bessel function. A graphical representation of the kernel function $F(px_{12})$, is given in Fig. 2. We shall use Eq. (12) and (13) and Fig. 2 in discussing the loss of spatial coherence due to scattering by the temperature microstructure.

Equation (12) indicates that the entire one-dimensional power spectrum contributes to a degree to determining the coherence at any given separation distance. However, we would now like to show that all portions of the power spectrum do not contribute to the same degree to determining the coherence for a given separation distance. Rather, it is possible to identify a limited portion of the power spectrum as being dominant in determining the coherence for a given separation distance. The specific portion that is dominant will be shown to depend on the separation distance. These conclusions are crucial for the theoretical results represented by Eq. (12) to be of much value and they are crucial for the subsequent development of a more computationally useful acoustic model.

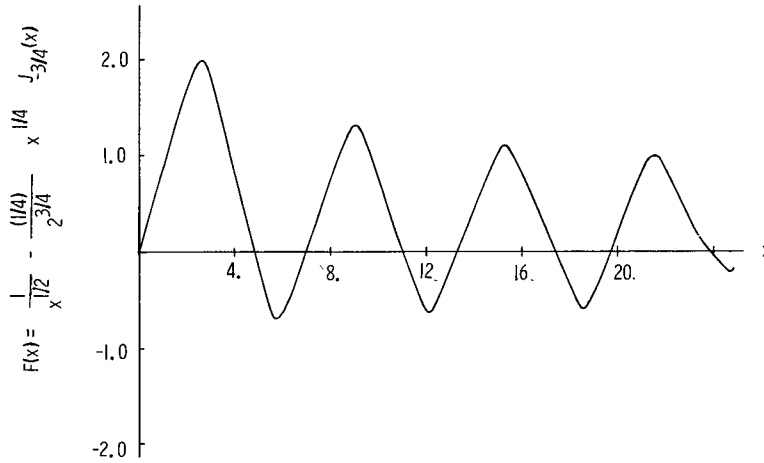


Fig. 2 — Kernel of integral that relates signal coherence to fluctuation power spectrum

Presenting the arguments that lead to the desired conclusions require that we have a visualization of a typical power spectrum. We present Fig. 3 and note the presence of two characteristic wave numbers (p_M, p_m) that span the correlation lengths within which most of the energy is contained. Typically, $p_M^{-1} \gg p_m^{-1}$. (In the ocean, estimates of p_M^{-1} range upward from several tens of kilometers, while p_m^{-1} could be as small as meters or less.) The power spectrum decreases monotonically, from its maximum value at p_M , with increasing p . The range of values between its maximum and the value at its high wave number cutoff is, typically, several orders of magnitude. Exterior to the range $p_M^{-1} > p^{-1} > p_m^{-1}$, we shall assume the falloffs to be rapid enough that we can treat these values as cutoff values.

The relationship between signal coherence, separation distance, and $\Phi_1(p)$ is given by the integral in Eq. (12). We shall interpret the role of the separation distance, in determining the value of this integral, as one of setting the scale factor for viewing $F(px_{12})$ as a function of p , the variable over which the integration is to be taken. Thus, decreasing x_{12} is interpreted as stretching the abscissa for viewing F as a function of p (see Fig. 4). We now incorporate this interpretation of the role of x_{12} , our visualization of a typical power spectrum, and the graphical representation that shows $F(px_{12})$ to be a decaying oscillatory function of px_{12} and construct the following qualitative description of the scattering. Consider a value of $x_{12} = 2.5p_M^{-1}$, which corresponds to a separation distance approximately equal to $\ell_{HM}/2.5$ where ℓ_{HM} is the maximum horizontal correlation length. For this separation distance, the first maximum of $F(px_{12})$ occurs at $p = p_M$, which is the location of the $\Phi_1(p)$ maximum. This situation is illustrated schematically in Fig. 4a. From this figure, it is clear that the dominant contributions to the integral come, for this separation distance, from values of p in the vicinity of $p = p_M$. For values of x_{12} that are smaller than $2.5 p_M^{-1}$, the first maximum of F occurs at a value $p > p_M$ (see Fig. 4b), indicating that the larger p values (smaller correlation lengths) will play a more significant role for smaller values of x_{12} . Further, we note that the monotonic

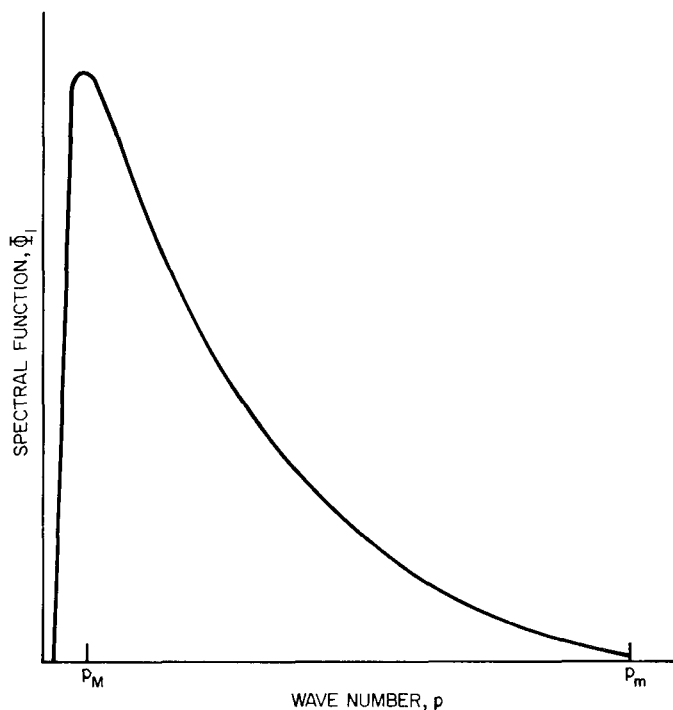


Fig. 3 — Schematic representation of temperature spectrum

decrease of $F(px_{12})$ from the first maximum with decreasing p indicates that the role of the larger size scale fluctuations (i.e., smaller wave number values) will lessen with decreasing x_{12} . Whether the role of the low-wave-number spectral components will be completely suppressed for small separation distances can be determined only by comparing the relative rates of the decrease of $\Phi_1(p)$ and the increase in $F(px_{12})$ with increasing p . For a simple power law behavior for $\Phi_1(p)$, $\Phi_1(p) \approx Ap^{-n}$, where A is a constant; the contribution of the lower wave numbers will be suppressed for small enough wave-number values if $n < 2.5$. In summary, then, we can conclude that, for a given separation distance, there is an upper wave number limit (of the order of $2.5 x_{12}$) to that portion of the refractive index spectrum that offers a significant contribution to the signal coherence. The question as to whether there is also a lower wave-number limit depends on the rate of falloff of $\Phi_1(p)$ with increasing p . For falloffs whose rates are less than $p^{-2.5}$, a lower limit is also indicated. This presence of a lower limit is fortunate for studies in ocean acoustics because most of the reported data (and the theories that have been presented in explanation) on the dependence of $\Phi_1(p)$ with p for small p values, i.e., large size scales, exhibit a falloff that is a good deal slower than $p^{-2.5}$. This would indicate that detailed information of these very large scale variations is not needed for estimating signal coherence at the smaller separation distances.

We now intend to develop a more computationally useful model than that given by Eq. (12) by introducing a specific functional form for $\Phi_1(p)$. The form should, hopefully,

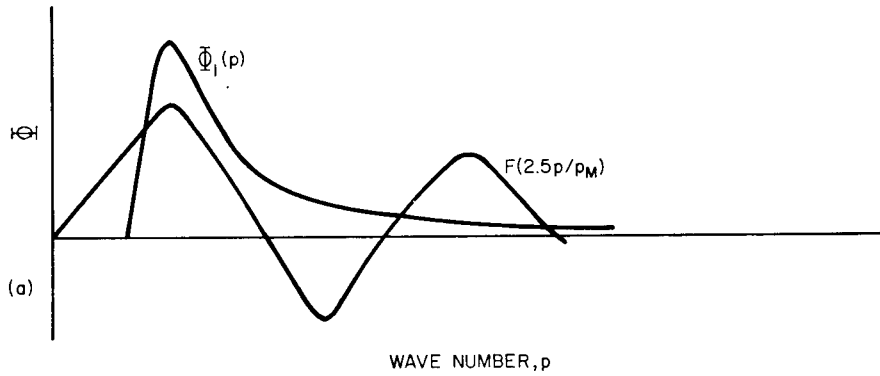


Fig. 4a — Schematic line graphs to demonstrate the effect of changing the separation distance on the kernel function in Eq. (10). $x_{12} = 2.5/p_M \approx 0.4 \ell_M$.

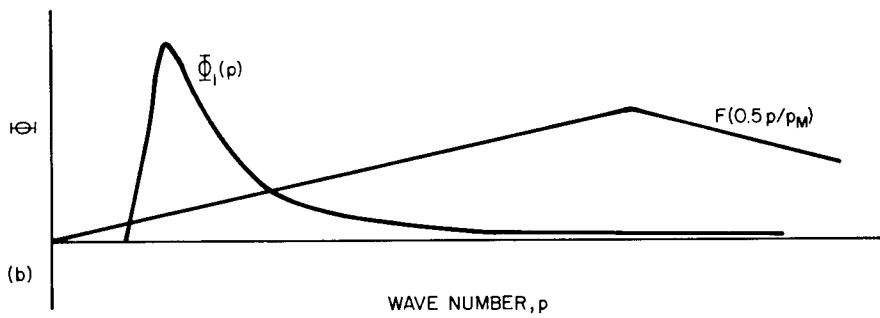


Fig. 4b — Schematic line graphs to demonstrate the effect of changing the separation distance on the kernel function in Eq. (10). $x_{12} = 0.5/p_M \approx 0.08 \ell_M$.

possess some degree of universality; i.e., it should be able to reproduce a variety of experimental results for an important class of environmental situations. Specification of $\Phi_1(p)$ would then be accomplished by specifying a limited number of parameters, which might be termed environmental parameters. These environmental parameters should be measurable under field conditions. Finally, it would be extremely advantageous to be able to justify a functional form that renders an analytic evaluation of the intergral. An example of a useful functional form is given by

$$\Phi_1(p) = \begin{cases} \frac{A_n^2}{(p^2 + p_M^2)^n} & p \leq p_m \\ 0 & p > p_m \end{cases} \quad (14)$$

where $p_M^{-1} \gg p_m^{-1}$.

Here, A_n and n are constants. This assumed form for $\Phi_1(p)$ gives a simple power law variation for $p_M^{-1} \gg p^{-1} \gg p_m^{-1}$. It also contains the high wave number cutoff at $p = p_m$ that was described in the typical spectrum. Further, it replaces a more realistic low-wave-number cutoff with a leveling off. This step is necessitated by the desire to obtain an analytic evaluation of the integral in Eq. (12). Our previous discussion further indicates that the replacement will not cause serious error for separation distances that satisfy $p_M^{-1} \gg x_{12}$ if $n < 5/4$. Introducing Eq. (14) into the integral, we find that the integration can be carried out, provided $x_{12} \gg p_m^{-1}$. We present, here, the following expression obtained for $n = 1$; i.e., a -2 power law:

$$\begin{aligned} \bar{\sigma}_2(0, 0) - \bar{\sigma}_2(x_{12}, 0) = 0.641 A_2^2 \bar{k}^{5/2} \ell_{yM} \left[\frac{1.216}{p_M^{3/2}} \right. \\ \left. - 1.19 \left(\frac{x_{12}}{p_M} \right)^{3/4} K_{3/4}(p_M x_{12}) \right]. \end{aligned} \quad (15)$$

Here, $K_{3/4}$ is a modified Bessel function. Eq. (15) can be considerably simplified by now introducing the restriction on the separation distance to values $x_{12} \ll p_M^{-1}$. The simplification is then accomplished by expanding the Bessel function as a power series and in truncating after a single term. Thus, we obtain

$$\bar{\sigma}_2(0, 0) - \bar{\sigma}_2(x_{12}, 0) = 1.1 A_2^2 \ell_{yM} \bar{k}^{5/2} x_{12}^{3/2} \quad (16)$$

Use of Eq. (16) in Eq. (12) leads to the following extremely simple expression relating signal coherence to signal wavelength, range, horizontal separation distance, and environmental parameters:

$$\left\{ \hat{\Gamma}(S, 0, R) \right\} = \hat{I} \exp(-E S^{3/2} R), \quad (17)$$

where $E = 1.1 A_2^2 \ell_{yM}$ is a nondimensional environmental parameter, $S = \bar{k} x_{12}$ is the nondimensional separation distance, and $R = \bar{k} z$ is the nondimensional range. The environmental parameter is expressed here in terms of measurable field data of the refractive-index fluctuations. In terms of temperature fluctuations data it is necessary to introduce a scale change for the A_2^2 term. Thus, we write,

$$E = 4.4 \left(\frac{1}{c} \frac{\partial c}{\partial T} \right)^2 A_T^2 \ell_{yM}$$

where A_T^2 is a parameter taken from temperature data and T is the temperature. For $T \approx 15^\circ\text{C}$, a salinity content of 36 ppm, experimental data indicate

$$\frac{1}{c} \frac{\partial c}{\partial T} \approx 2 \times 10^{-3} / ^\circ\text{C},$$

which leads to

$$E = 1.76 \times 10^{-5} A_T^2 \ell_{yM}$$

where A_T^2 is to be expressed in units of $(^\circ\text{C})^2/\text{length}$.

A characteristic coherence length can be defined somewhat arbitrarily by the condition that it be the separation at which the coherence falls to $1/e$ of the zero separation value. We write,

$$L_x = E^{-2/3} R^{-2/3} \quad (18)$$

where $L_x = k\ell_x$ is the nondimensional coherence length. In Fig. 5 we present plots of L_x as functions of R on a log-log scale for several values of E that might be encountered

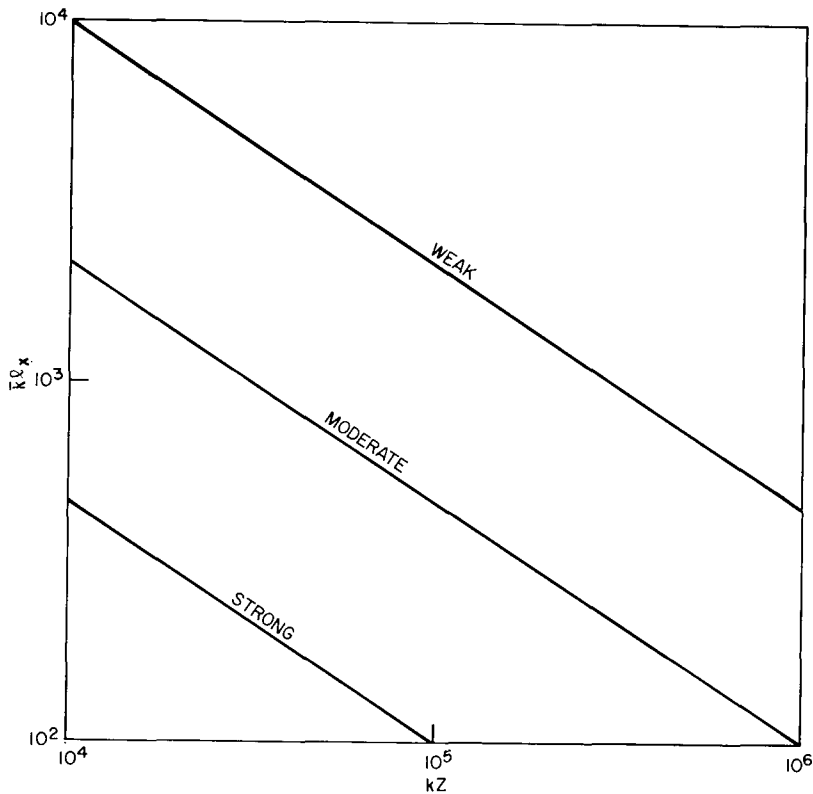


Fig. 5 — Nondimensional signal coherence length L_x as a function of the nondimensional range R

in the ocean. The E values chosen correspond to an ℓ_{yM} value of the order of 10 m, and the A_T^2 values were chosen to encompass the reported data (see Appendix C). Thus, $E = 10^{-8}$ corresponds to what might be termed a strong fluctuational field, $E = 10^{-9}$ to a moderate field, and $E = 10^{-10}$ to a weak field.

It is well to emphasize at this point that all results starting with Eq. (15) depend on the validity of the -2 power law as a representation of $\Phi_1(p)$. In Appendix C we consider this question in considerable detail from both an experimental and a theoretical point of view. We also present the results of a numerical study that was carried out by using the presently available best estimates of $\Phi_1(p)$. Further, we compare these numerical results to corresponding values obtained by using a simple -2 power law. In all the cases considered, the -2 power law estimates were definitely acceptable. Thus, for the range of environmental parameters considered, Eqs. (16) through (18) can be expected to give valid estimates of signal coherence for separation distances that range from values of the order of 100 or less to values of the order of 1 or 2 km.

We conclude this discussion of the loss of spatial coherence due to scattering by the temperature microstructure by considering the effects of diffraction, refraction, and inhomogeneous statistics for the fluctuating field. In Appendix D we consider these questions in some detail. Here we shall list some of the highlights of that more detailed discussion. Refraction effects result from the presence of a depth-dependent mean sound speed. In Appendix D we show that the presence of a depth-dependent mean sound speed has no effect on the averaged azimuthal scattering. (Average here refers to an average over the depth coordinate.) The potential effects of depth-dependent statistics for the temperature microstructure are far more significant. One cannot, in general, average out the effects of these on the azimuthal scattering. If, however, the acoustic signal followed a single propagation path, or, if the multipath structure is such that the fluctuations encountered over the different multipaths are statistically similar, then one can remove the effects of depth-dependent statistics on azimuthal scattering by averaging over the depth coordinate. Diffraction effects enter if the initial radiation is not a plane wave. Previous work that has appeared in the optics literature leads to the conclusion that the characteristic correlation length L_x for nonplanar initial conditions differs from that for the plane wave case by a factor of the order of 1 to 3. In all cases the plane wave case gives an underestimation of the characteristic correlation length. The effects of diffraction, refraction, and inhomogeneous statistics on azimuthal scattering as measured at a fixed depth are much more difficult to ascertain and are left for a future investigation.

CONCLUSIONS AND RECOMMENDATIONS

We repeat the more significant results and conclusions of our study and present recommendations for future courses of actions.

1. The limitations on vertical resolution, which are due to the temperature microstructure, will be much greater than corresponding limitations on horizontal resolution.
2. In the multiscatter region, horizontal resolution is affected by the statistics of the temperature microstructure measured along a vertical line. The theory identifies a

characteristic correlation length, measured in the depth direction, which is an important factor in controlling the azimuthal scattering. Thus, we recommend the gathering of more data that would reveal the dependence of the spatial correlation of the fluctuating temperature field on separation measured in the depth direction.

3. Horizontal resolution in the multiscatter region is affected to some degree by all size-scale temperature fluctuations measured in a horizontal plane. The degree to which a specified size scale affects this resolution depends on factors such as strength of microstructure, range, and acoustic frequency. The theory indicates that for ranges of 500 to 1,000 n. mi., for a frequency range of 100 to 300 Hz, and for microstructures of the strength commonly encountered, the larger size scale fluctuations that are presently attributed to the presence of internal waves have a dominant effect on resolution. The smaller size fluctuations that are attributed to ocean turbulence will be important for much longer ranges or, for much higher frequencies. We recommend, therefore, that future studies of the temperature microstructure concentrate on larger horizontal size-scale fluctuations than have been studied in the past.

4. A depth-dependent horizontal temperature spectrum could have a significant effect on horizontal resolution. Because theoretical considerations and some experimental data show the importance of the Brunt-Väisälä frequency profile in controlling this spectrum, an improved acoustic model that incorporates these data is desirable. A theoretical basis for incorporating the effects of depth-dependent statistics, together with the effects of diffraction and refraction, is provided in Appendix D. We recommend that an acoustic model based on this theory be implemented.

5. The present report does not explicitly consider the potential utility of the vertical resolution of a billboard array in isolating multipaths. It seems clear, however, that the isolation of a single multipath could affect horizontal resolution in one of two situations. The first situation occurs when the two multipaths are so close that the acoustic signals that traverse them encounter essentially identical microstructure fields. The scattered wave energies for the two multipaths could be expected to be strongly correlated in this case. Interference effects might then be expected to affect horizontal resolution. In the second situation the two multipaths are of widely differing orders, or are such that the acoustic signals that traverse them encounter microstructure fields that even differ widely in a statistical sense. The azimuthal scattering of the signals that traverse the two multipaths would differ in this case. The importance of either of these situations can be studied using the extended theory that we recommended previously.

6. While the end results of the derivation are contained in some surprisingly simple equations, the derivation itself is highly complex. Accordingly, it is important that an experimental program designed to test the acoustic models be undertaken, and this we recommend.

Appendix A

SINGLE SCATTER SOLUTION

A simple way to determine the angular spectrum resulting from the scattering of a plane wave by a random medium is to consider the geometry, given in Fig. A1.

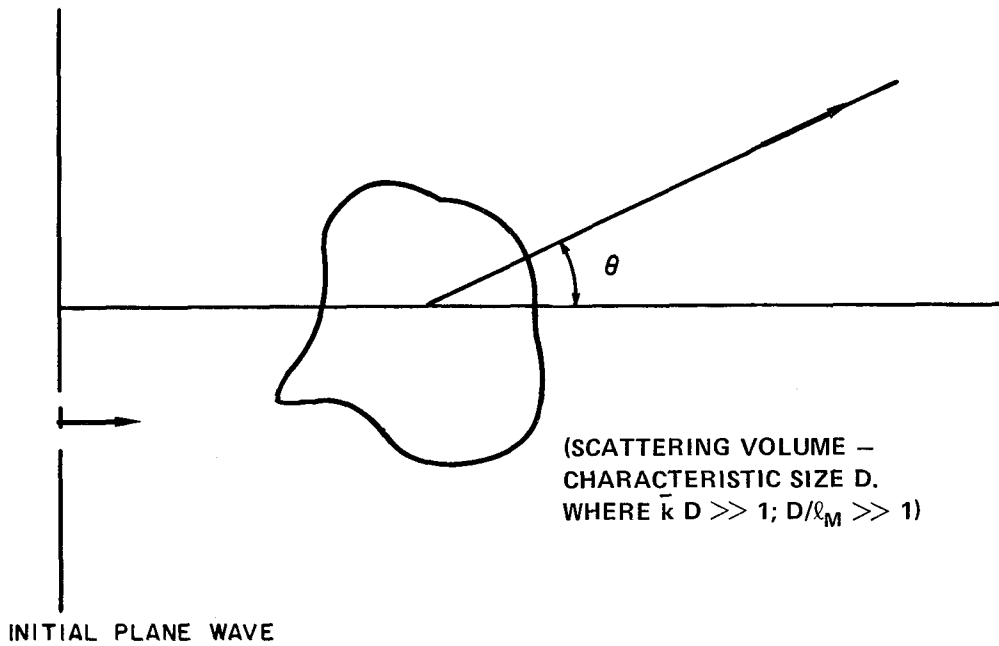


Figure A1

A time-harmonic plane wave impinges on a finite scattering volume. We calculate the intensity of the scattered radiation at a very distant point (R, θ) where $R \gg \bar{k}D^2$. For an isotropic random medium we find the well-known result that scattering angles θ are limited to

$$\theta = O\left(\frac{1}{\bar{k} \ell_m}\right)$$

if $\bar{k} \ell_m \gg 1$; that is,

$$\{\hat{I}_s(R, \theta)\} \approx O,$$

for

$$\theta \gg \frac{1}{\bar{k} \ell_m}$$

where \hat{I}_s is the intensity of the scattered radiation. On the other hand, $\{\hat{I}_s(R, \theta)\}$ is independent of θ if $\bar{k} \ell_m \ll 1$. In the present study we are interested in an anisotropic medium with different characteristic correlation lengths associated with differing directions. We thus have three pairs of lengths (ℓ_{xM}, ℓ_{xm}) , (ℓ_{yM}, ℓ_{ym}) and (ℓ_{zM}, ℓ_{zm}) . We shall study combinations of conditions to show the nature of the problem, but in this appendix we shall be particularly interested in the case $\bar{k}\ell_{yM} \ll 1$, $\bar{k}\ell_{xm} \gg 1$, $\bar{k}\ell_{zm} \gg 1$. Here we will find that scattering is significant only where

$$\theta_x = O\left(\frac{1}{\bar{k}\ell_{zm}}\right)$$

$$\theta_y = O\left[\left(\frac{1}{\bar{k}\ell_{zm}}\right)^{1/2}\right]$$

The angle θ_x is measured in a horizontal plane; θ_y is measured in a vertical plane.

The equation governing the propagation of a pressure signal in water with a variable index of refraction is taken to be

$$\nabla^2 p = \frac{1}{c^2(\mathbf{x})} \frac{\partial^2 p}{\partial t^2} \tag{A1}$$

where $p(\mathbf{x}, t)$ is the pressure field and $c^2(\mathbf{x})$ is the variable speed of sound. There are a number of approximations* necessary to obtain Eq. (A1). In particular we choose here $c^2(\mathbf{x})$ rather than $c^2(\mathbf{x}, t)$ because we will use ensemble averaging and can choose the properties of the water to be fixed in each realization of the ensemble. It is convenient to rewrite Eq. (A1) as

*L. Chernov, *Wave Propagation in a Random Medium*, McGraw-Hill, New York 1960.

$$\nabla^2 p = \frac{\{n^2\}}{\{c\}^2} \left[1 + \epsilon \mu(\mathbf{x}) \right] \frac{\partial^2 p}{\partial t^2} \quad (\text{A2})$$

where the braces $\{ \}$ indicate an ensemble average. The term $\{c\}$ is the mean sound speed and $\mu(\mathbf{x})$ denotes a centered stochastic process of unit variance defined by the randomly varying index-of-refraction field. The term $\{n^2\}$ is given by

$$\{n^2\} = \{c\}^2 / \{c^2\}, \quad (\text{A3})$$

and ϵ is a measure of the strength of the index-of-refraction fluctuation field. In all of our studies we shall assume that $\epsilon \ll 1$. To first order in ϵ , $\{n^2\} = 1$. Therefore we can replace the $\{n^2\}$ in Eq. (A2) by 1.

For narrowband signals with central frequency $\bar{\nu}$ it is convenient to introduce the approximation

$$p(\mathbf{x}, t) = \text{Re} \left[\hat{p}(\mathbf{x}, \bar{\nu}) \exp(2\pi i \bar{\nu} t) \right] \quad (\text{A4})$$

where $\hat{p}(\mathbf{x}, \bar{\nu})$ is the complex pressure field. Substitution into Eq. (A2) yields

$$\nabla^2 \hat{p} + \bar{k}^2 \left[1 + \epsilon \mu(\mathbf{x}) \right] \hat{p} = 0 \quad (\text{A5})$$

where

$$\bar{k} = 2\pi \bar{\nu} / \{c\} \quad (\text{A6})$$

The single scatter solutions are obtained by writing the solution in the form

$$\hat{p}(\mathbf{x}) = \hat{p}_0(\mathbf{x}) + \epsilon \hat{p}_1(\mathbf{x}) \quad (\text{A7})$$

where $\hat{p}_0(\mathbf{x})$ and $\hat{p}_1(\mathbf{x})$ are independent of ϵ and where all terms proportional to ϵ^2 and to higher powers of ϵ have been dropped. The $\bar{\nu}$ argument has been suppressed. For an initial plane wave incident on the scattering volume we have

$$\hat{p}_0(\mathbf{x}) = (\hat{I})^{1/2} \exp(i\bar{k}z) \quad (\text{A8})$$

whereas $\hat{p}_1(\mathbf{x})$ satisfies the equation

$$\begin{aligned} \nabla^2 \hat{p}_1 + \bar{k}^2 \hat{p}_1 &= -\bar{k}^2 \mu(\mathbf{x}) p_0(\mathbf{x}) \\ &= -\bar{k}^2 \mu(\mathbf{x}) (\hat{I})^{1/2} \exp(i\bar{k}z). \end{aligned} \quad (\text{A9})$$

In Eq. (A8), \hat{I} might be termed the intensity of the initial plane wave, although this definition differs slightly from the usual definition in acoustics studies. The solution of Eq. (A9) is to satisfy the radiation condition far from the scattering volume and we write the result as

$$\hat{p}_1(\mathbf{x}) = \frac{-\bar{k}^2 \hat{I}^{1/2}}{4\pi} \int \frac{\exp(i\bar{k}[r(\mathbf{x}, \mathbf{x}') + z']]}{r(\mathbf{x}, \mathbf{x}')} \mu(\mathbf{x}') d\mathbf{x}' \quad (\text{A10})$$

where $r(\mathbf{x}, \mathbf{x}')$ is the distance between \mathbf{x} and \mathbf{x}' . The integration is over the scattering volume.

Defining the intensity of the scattered radiation field by

$$\{\hat{I}_S(\mathbf{x})\} = \epsilon^2 \{\hat{p}_1(\mathbf{x}) \hat{p}_1^*(\mathbf{x})\}. \quad (\text{A11})$$

one obtains the following expression for $\{\hat{I}_S\}$:

$$\begin{aligned} \{\hat{I}_S(\mathbf{x})\} &= \frac{\bar{k}^4 \hat{I}}{(4\pi)^2} \iint \frac{\exp\{i\bar{k}[r(\mathbf{x}, \mathbf{x}') - r(\mathbf{x}, \mathbf{x}'') + (z' - z'')]\}}{r(\mathbf{x}, \mathbf{x}') r(\mathbf{x}, \mathbf{x}'')} = \\ &\quad \times \sigma(\mathbf{x}', \mathbf{x}'') d\mathbf{x}' d\mathbf{x}'' \end{aligned} \quad (\text{A12})$$

where

$$\sigma(\mathbf{x}', \mathbf{x}'') = \epsilon^2 \{\mu(\mathbf{x}') \mu(\mathbf{x}'')\} \quad (\text{A13})$$

is the spatial correlation function σ defined on the index-of-refraction fluctuations.

Introducing homogeneous statistics and the far field approximation enables us to accomplish a partial integration* of the right-hand side of Eq. (A12). We write the result

$$\{\hat{I}_S(\mathbf{x})\} = \frac{\bar{k}^4 \hat{I}}{(4\pi)^2 R^2} \int \sigma(\mathbf{u}) \exp\left[-i\bar{k}\left(\frac{\mathbf{u} \cdot \mathbf{x}}{R} - u_z\right)\right] d\mathbf{u} \quad (\text{A14})$$

where $\mathbf{u} = \mathbf{x}' - \mathbf{x}''$ is the difference coordinate. We shall make use of Eq. (A14) to demonstrate the dependence of the angular variation of the scattered intensity on correlation lengths defined by the index-of-refraction fluctuation field.

Toward this end we use a sample correlation function $\sigma(\mathbf{u})$ of the following form

$$\sigma(\mathbf{u}) = \sigma_0 \exp\left[-\left(\frac{u_x^2}{\ell_x^2} + \frac{u_y^2}{\ell_y^2} + \frac{u_z^2}{\ell_z^2}\right)\right] \quad (\text{A15})$$

(We emphasize that Eq. (A15) is not meant to give a realistic description of the index-of-refraction fluctuation field that is caused by the ocean temperature microstructure but is introduced only to provide the insight we require.)

*M. J. Beran and G. B. Parrent, Jr., *Theory of Partial Coherence*, Prentice-Hall Inc., Englewood Cliffs, N. J., 1964.

Substituting Eq. (A15) into Eq. (A14) and integrating yields

$$\left\{ \hat{I}_S(\mathbf{x}) \right\} = \frac{\sigma_0 \bar{k}^4 \hat{I}V}{(4\pi)^2 R^2} \pi^{3/2} \ell_x \ell_y \ell_z \exp \left\{ \frac{-\bar{k}^2}{4} \left[\frac{\ell_x^2 x^2}{R^2} + \frac{\ell_y^2 y^2}{R^2} + \ell_z^2 \left(1 - \frac{z}{R} \right)^2 \right] \right\}. \quad (\text{A16})$$

In spherical coordinates; i.e. $x = R \sin \theta \cos \varphi$, $y = R \sin \theta \sin \varphi$, $z = R \cos \theta$,

$$\left\{ \hat{I}_S(\mathbf{x}) \right\} = \frac{\sigma_0 \bar{k}^4 \hat{I}V}{(4\pi)^2 R^2} \pi^{3/2} \ell_x \ell_y \ell_z \exp \left\{ \frac{-\bar{k}^2}{4} \left[\left(\ell_x^2 \cos^2 \varphi + \ell_y^2 \sin^2 \varphi \right) \sin^2 \theta + \ell_z^2 (1 - \cos \theta)^2 \right] \right\}. \quad (\text{A17})$$

Now consider a few possibilities:

$$(i) \ell_x = \ell_y = \ell_z = \ell \quad \text{where } \bar{k} \ell \gg 1$$

This case is the usual one discussed in atmospheric propagation studies. Here

$$\left\{ \hat{I}_S^A(\mathbf{x}) \right\} = \frac{\sigma_0 \bar{k}^4 \hat{I}V}{(4\pi)^2 R^2} \pi^{3/2} \ell^3 \exp \left[\frac{-\bar{k}^2 \ell^2}{2} (1 - \cos \theta) \right] \quad (\text{A18})$$

where $\left\{ \hat{I}_S^A(\mathbf{x}) \right\}$ is $\left\{ \hat{I}_S(\mathbf{x}) \right\}$ for this case. Thus, $\left\{ \hat{I}_S^A(\mathbf{x}) \right\}$ is appreciable only if $(1 - \cos \theta) \ll 1$. Therefore

$$1 - \cos \theta \approx \frac{\theta^2}{2}$$

and

$$\theta = O\left(\frac{1}{\bar{k}\ell}\right) \quad (\text{A19})$$

for scattering intensities of significant strength.

$$(ii) \ell_x = \ell_y = \ell_z = \ell \quad \text{where } \bar{k}\ell \ll 1.$$

In this case all correlation lengths are small compared to the radiation wavelength. Here,

$$\left\{ \hat{I}_S^B(\mathbf{x}) \right\} = \frac{\sigma_0 \bar{k}^4 \hat{I}V}{(4\pi)^2 R^2} \pi^{3/2} \ell^3, \quad (\text{A20})$$

and the scattering is isotropic.

$$(iii) \ell_x = \ell_z; \bar{k} \ell_x \gg 1; \bar{k} \ell_y \ll 1$$

This is the case of interest in this paper. The vertical direction is the y direction. Here,

$$\left\{ \hat{I}_S^C(\mathbf{x}) \right\} = \frac{\sigma_0 \bar{k}^4 \hat{I}V}{(4\pi)^2 R^2} \pi^{3/2} \ell_x^2 \ell_y \exp \left\{ \frac{\bar{k}^2}{4} \ell_x^2 \left[\cos^2 \varphi \sin^2 \theta + (1 - \cos \theta)^2 \right] \right\} \quad (\text{A21})$$

where $\hat{I}_S^C(\mathbf{x})$ is the scattering intensity in this case. Scattering in the vertical direction is investigated by choosing a position where $\cos \varphi = 0$. We find that

$$\left\{ \hat{I}_S^C(y) \right\} = \frac{\sigma_0 \bar{k}^4 \hat{I}V}{(4\pi)^2 R^2} \pi^{3/2} \ell_x^2 \ell_y \exp \left[\frac{-\bar{k}^2 \ell_x^2}{4} (1 - \cos \theta)^2 \right]. \quad (\text{A22})$$

For the exponential term to be appreciable we must have

$$(1 - \cos \theta)^2 \ll 1.$$

Therefore we obtain for the vertical scattering angle $\theta = \theta_V$,

$$\frac{\bar{k}^2 \ell_x^2}{4} \frac{\theta_V^4}{4} = O(1)$$

and

$$\theta_V = O\left(\frac{1}{(\bar{k}\ell_x)^{1/2}}\right).$$

Scattering in the transverse horizontal direction is investigated by choosing a position $y = R \sin \varphi = 0$ or $\cos \varphi = 1$. Equation (A21) is then

$$\left\{ \hat{I}_S^C(x) \right\} = \frac{\sigma_0 \bar{k}^4 \hat{I}V}{(4\pi)^2 R^2} \ell_x^2 \ell_y \exp \left[\frac{-\bar{k}^2 \ell_x^2}{2} (1 - \cos \theta) \right]. \quad (\text{A24})$$

This is similar to the first case and yields, for the horizontal scattering angle $\theta = \theta_H$,

$$\theta_H = O\left(\frac{1}{\bar{k}\ell_x}\right), \quad (\text{A25})$$

for the scattering to be appreciable.

Examination of the results of the third case shows that for single scattering we may expect that the horizontal angular spread will be of the order of $(1/\bar{k}\ell_x)$ while the vertical spread will be of the order of $(1/\bar{k}\ell_x)^{1/2}$. The same type of analysis holds in general for an arbitrary function $\sigma(\mathbf{u})$. We only require that $\bar{k}\ell_{yM} \ll 1$ and $\bar{k}\ell_{kM} \gg 1$. The statement that $\theta = O(1/\bar{k}\ell_{xm})$ means that scattering from the smallest scale fluctuations gives $\theta = O(1/\bar{k}\ell_{xm})$. The largest scales give $\theta = O(1/\bar{k}\ell_{xM})$. Since, however, $\bar{k}\ell_{xM} > \bar{k}\ell_{xm}$, we usually use only the order of magnitude associated with $\bar{k}\ell_{xm}$.

For the case $\bar{k}\ell_{yM} = O(1)$, including the case where $\bar{k}\ell_{yM} \ll 1$, similar analysis shows $\theta_V = O(\theta_M)$, for the scattering to be appreciable where

$$\frac{1}{\bar{k}\ell_{xm}} < \theta_M < \left(\frac{1}{\bar{k}\ell_{xm}} \right)^{1/2}$$

The important fact is that when $\bar{k}\ell_{xm} \gg 1$, we find θ is no greater than $O[1/(\bar{k}\ell_{xm})^{1/2}]$ for all values of $\bar{k}\ell_{yM}$.

The results given in Eqs. (A23) and (A25) are valid only for single scattering but we shall see in Appendix B how these results motivate approximations that allow us to solve the multiple scattering problem.

Appendix B

MULTIPLE SCATTER SOLUTION

In this appendix we study the mutual coherence function $\{\Gamma\}$ given by Eq. (1), which we repeat here:

$$\left\{ \hat{\Gamma}(\mathbf{x}_1, \mathbf{x}_2, \bar{\nu}) \right\} = \left\{ \hat{p}(\mathbf{x}_1, \bar{\nu}) \hat{p}(\mathbf{x}_2, \bar{\nu}) \right\}. \quad (1)$$

Again, \mathbf{x}_1 and \mathbf{x}_2 are the two positions of interest and $\bar{\nu}$ is the central frequency of the narrowband signal. The quantity $\hat{p}(\mathbf{x})$ is the complex acoustic pressure at point \mathbf{x} . The random medium is confined to the half-space, $z > 0$. Homogeneous statistics are assumed. The problem of a plane-wave radiation field incident from $z \rightarrow \infty$ is considered. Using the results of the last section we neglect any backscattered radiation, which enables our writing the following expression for $\{\Gamma\}$ for two points in the half space $z < 0$.

$$\left\{ \hat{\Gamma}(\mathbf{x}_1, \mathbf{x}_2, \bar{\nu}) \right\} = I \exp i\bar{k}(z_1 - z_2) \quad z_1, z_2 < 0. \quad (B1)$$

By virtue of the restriction to homogeneous statistics, the general solution in the half space $z > 0$ is of the form

$$\left\{ \hat{\Gamma}(x_{12}, y_{12}, z_{12}, z, \bar{\nu}) \right\}$$

where $x_{12} = x_2 - x_1$, $y_{12} = y_2 - y_1$, $z_{12} = z_2 - z_1$, $z = z_1$. We are not interested in the general solution, however, and shall only determine the mutual coherence function measured at two points in the same plane normal to the original plane wave direction; i.e., for two points where $z_{12} = 0$. It is this quantity that gives a measure of the resolution limitation resulting from the presence of the random medium.

A single scatter solution of the posed problem is immediately afforded by Eq. (A10). It is well appreciated, however, that the validity of the solution so obtained has a range dependence and that a procedure for incorporating multiple scattering effects is necessary for longer propagation distances. In this section we use the procedure of M. J. Beran [B1].

In carrying out the solution, the region between 0 and z is divided by a series of $M-1$ infinite planes located at the coordinates $\Delta z, 2\Delta z, \dots, (M-1)\Delta z$, where $\Delta z = z/M$. The number M is chosen large enough so that in the interval $j\Delta z$ and $(j+1)\Delta z$, $\left\{ \hat{\Gamma}(\mathbf{x}_1, \mathbf{x}_2) \right\}$ can be obtained from its value measured on $z_1 = z_2 = j\Delta z$ using a single scatter approximation. The $\bar{\nu}$ argument in $\{\Gamma\}$ is suppressed. Thus, one can show that in this interval

$$\left\{ \hat{\Gamma}_S(\mathbf{x}_1, \mathbf{x}_2) \right\} = \frac{\bar{k}^4}{(4\pi)^2} \iint \frac{\exp(i\bar{k}[r(\mathbf{x}_1, \mathbf{x}') - r(\mathbf{x}_2, \mathbf{x}'')]}{r(\mathbf{x}_1, \mathbf{x}') r(\mathbf{x}_2, \mathbf{x}'')} \times \sigma(\mathbf{x}', \mathbf{x}'') \left\{ \hat{\Gamma}_{j\Delta z}(\mathbf{x}', \mathbf{x}'') \right\} d\mathbf{x}' d\mathbf{x}'' \quad (B2)$$

In this equation $\{\hat{\Gamma}_S(\mathbf{x}_1, \mathbf{x}_2)\}$ is the scattered portion of $\{\hat{\Gamma}(\mathbf{x}_1, \mathbf{x}_2)\}$, and $\{\hat{\Gamma}_{j\Delta z}(\mathbf{x}', \mathbf{x}'')\}$ is the mutual coherence function that exists in the interval $j\Delta z < z < (j+1)\Delta z$ when there is no scattering in this interval. The integrations are over the region between the planes located at $z = j\Delta z$ and $z = (j+1)\Delta z$. Eq. (B2) is equivalent to Eq. (7) in the work of Beran [B1].

In writing Eq. (B2) we have assumed that $\mu(\mathbf{x}')\mu(\mathbf{x}'')$ and $\{\hat{\Gamma}_{j\Delta z}(\mathbf{x}', \mathbf{x}'')\}$ are uncorrelated in the interval $j\Delta z < z < (j+1)\Delta z$. This assumption is valid if we require that $\Delta z \gg \lambda_{zM}$. If $\Delta z \gg \lambda_{zM}$, then $\mu(\mathbf{x}')$ and $\mu(\mathbf{x}'')$ for $z', z'' > j\Delta z$ are uncorrelated to $\mu(\mathbf{x})$ for $z < j\Delta z$ over most of the interval. On the other hand, $\{\hat{\Gamma}_{j\Delta z}(\mathbf{x}', \mathbf{x}'')\}$ is only dependent on $\mu(\mathbf{x})$ for $z < j\Delta z$ since the scattering is in the forward direction. Therefore, to a good approximation, $\mu(\mathbf{x}')\mu(\mathbf{x}'')$ and $\{\hat{\Gamma}_{j\Delta z}(\mathbf{x}', \mathbf{x}'')\}$ may be assumed to be uncorrelated in the interval $j\Delta z < z < (j+1)\Delta z$.

It is desired to simplify the r.h.s. of Eq. (B2) based on the knowledge that the scattering is restricted to small angles. The procedure is the same as for the isotropic case, except that here, because $\theta_y = O[1/(k l_{zm})^{1/2}]$ rather than $O(1/k l_{zm})$, the small angle approximation is weaker and we must impose more stringent conditions than those given in the latter case.

An expansion and truncation of the expressions for $r(\mathbf{x}_1, \mathbf{x}')$ and $r(\mathbf{x}_2, \mathbf{x}'')$ yield simplified expressions that can be validly used provided we can show that the neglected terms are small. Thus, we approximate $r(\mathbf{x}_1, \mathbf{x}')$ in the exponent by

$$r(\mathbf{x}_1, \mathbf{x}') \approx z_1 - z' + \frac{1}{2} \frac{[(x_1 - x')^2 + (y_1 - y')^2]}{z_1 - z'} \quad (\text{B3})$$

and in the denominator by the single term $z_1 - z'$. This approximation is valid provided

$$\frac{(x_1 - x')^2 + (y_1 - y')^2}{(z_1 - z')^2} \ll 1 \quad (\text{B4})$$

and

$$\frac{\bar{k}[(x_1 - x')^4 + (y_1 - y')^4]}{(z_1 - z')^3} \ll 1 \quad (\text{B5})$$

The condition required by Eq. (B4) is satisfied if

$$\theta_x^2 \ll 1 \text{ and } \theta_y^2 \ll 1, \quad (\text{B6})$$

where θ_x and θ_y are the angular spreads measured at a generic point in the interval in the x and y directions, respectively. The results of Appendix A justify the assumption of small angle scattering incorporated in this condition. The condition required by Eq. (B5) is satisfied for all points in the interval $j\Delta z < z < (j+1)\Delta z$

$$\text{if } \bar{k}(\Delta z) \theta_x^4 \ll 1. \text{ and } \bar{k}(\Delta z) \theta_y^4 \ll 1$$

This condition can be interpreted as an upper bound limitation on the interval size (Δz). The results of the last section demonstrate that the second of the two conditions given will be the most difficult to satisfy. Based on the result that

$$\theta_y = O \frac{1}{(\bar{k}\ell_{zm})^{1/2}} \quad , \quad (\text{B8})$$

Eq. (B7) requires that

$$\frac{\Delta z}{k\ell_{zm}^2} \ll 1. \quad (\text{B9})$$

This condition, together with the condition that $\Delta z \gg \ell_{zM}$, requires that

$$\frac{\ell_{zM}}{\bar{k}\ell_{zm}^2} \ll 1. \quad (\text{B10})$$

We shall accept Eq. (B10) as a restriction on the theory being developed.

Substituting the simplified expressions for $r(\mathbf{x}_1, \mathbf{x}')$ and $r(\mathbf{x}_2, \mathbf{x}'')$ into Eq. (B2) and introducing the transformed coordinates

$$\begin{aligned} \mathbf{s} &= \mathbf{x}'' - \mathbf{x}' \\ \mathbf{p} &= \mathbf{x}' \end{aligned} \quad (\text{B11})$$

yield the following expression for $\left\{ \overset{\wedge}{\Gamma}_S(\mathbf{x}_1, \mathbf{x}_2) \right\}$:

$$\begin{aligned} \left\{ \overset{\wedge}{\Gamma}_S(\mathbf{x}_1, \mathbf{x}_2) \right\} &= \frac{\bar{k}^4}{(4\pi)^2} \exp [i\bar{k}(z_1 - z_2)] \iint \frac{\exp i\bar{k}s_z}{(z_1 - p_z)(z_2 - s_z - p_z)} \times \exp \\ &\left\{ \frac{i\bar{k}}{2} \left[\frac{(x_1 - p_x)^2 + (y_1 - p_y)^2}{z_1 - p_z} - \frac{(x_2 - s_x - p_x)^2 + (y_2 - s_y - p_y)^2}{z_2 - s_z - p_z} \right] \right\} \times \sigma(\mathbf{s}) \\ &\left\{ \overset{\wedge}{\Gamma}_{j\Delta z}(\mathbf{s}, p_z) \right\} ds dp. \end{aligned} \quad (\text{B12})$$

Next we wish to introduce the following simplified expressions into the exponent appearing in Eq. (B12):

$$\frac{(x_2 - s_x - p_x)^2}{z_2 - s_z - p_z} \approx \frac{(x_2 - s_x - p_x)^2}{z_2 - p_z} \quad (\text{B13})$$

and

$$\frac{(y_2 - s_y - p_y)^2}{z_2 - s_z - p_z} \approx \frac{(y_2 - s_y - p_y)^2}{z_2 - p_z} + \frac{s_z(y_2 - s_y - p_y)^2}{(z_2 - p_z)^2}. \quad (\text{B14})$$

Again, reference to the first term neglected, reveals that the condition given by Eq. (B13) requires, in addition to $\Delta z \gg \ell_{zM}$,

$$\frac{\bar{k} s_z (x_2 - s_x - p_x)^2}{(z_2 - p_z)^2} \ll 1,$$

which is satisfied if

$$\bar{k} \ell_{zM} \theta_x^2 \ll 1. \tag{B15}$$

Using the result of Appendix A that

$$\theta_x = O(1/\bar{k} \ell_{zm}),$$

Eq. (B15) leads to the condition already accepted; i.e. Eq. (B10).

To justify Eq. (B14), we must show that

$$\frac{\bar{k} s_z^2 (y_2 - s_y - p_y)^2}{(z_2 - p_z)^3} \ll 1.$$

This condition, in turn, requires that

$$\frac{\bar{k} \ell_{zM}^2 \theta_y^2}{\Delta z} \ll 1,$$

which is a more severe restriction on the formalism than $\Delta z \gg \ell_{zM}$. Using the order of magnitude estimate of θ_y , we write

$$\frac{\ell_{zM}^2}{(\Delta z) \ell_{zm}} \ll 1. \tag{B16}$$

This condition, together with Eq. (B9), leads to a more severe restriction than Eq. (B10); namely,

$$\frac{\ell_{zM}^2}{\bar{k} \ell_{zm}^3} \ll 1. \tag{B17}$$

We shall accept Eqs. (B16) and (B17) as restrictions on the theory.

Equations (B13) and (B14) are now introduced into Eq. (B12). In addition, we replace $z_2 - s_z - p_z$ in the denominator by $z_2 - s_z$, which is consistent with all of the approximations already introduced. The result is written

$$\begin{aligned}
 \left\{ \hat{\Gamma}_S(\mathbf{x}_1, \mathbf{x}_2) \right\} &= \frac{\bar{k}^4}{(4\pi)^2} \exp [i\bar{k}(z_1 - z_2)] \iint \frac{\exp i\bar{k} s_z}{(z_1 - p_z)(z_2 - p_z)} \\
 &\times \exp \left(\frac{i\bar{k}}{2} \left\{ \left[\frac{(x_1 - p_x)^2}{z_1 - p_z} - \frac{(x_2 - p_x - s_z)^2}{z_2 - p_z} \right] + \left[\frac{(y_1 - p_y)^2}{z_1 - p_z} - \frac{(y_2 - p_y - s_y)^2}{z_2 - p_z} \right. \right. \right. \\
 &\left. \left. \left. - \frac{s_z(y_2 - p_y - s_y)^2}{(z_2 - p_z)^2} \right] \right\} \right) \sigma(s) \left\{ \hat{\Gamma}_{j\Delta z}(s, \mathbf{p}) \right\} ds dp
 \end{aligned} \tag{B18}$$

We next set $z_1 = z_2 = z$. The integral over p_x can then be readily performed since the p_x^2 terms cancel. We find the factor $(2\pi/\bar{k})(z - p_z)\delta(s_x - x_{12})$ where δ is the Dirac delta function. The integral over p_y is more complex but after some manipulation we find the factor

$$(2\pi)^{1/2} \frac{(z - p_z)}{(\bar{k}|s_z|)^{1/2}} \exp \left(i\bar{k} \left\{ \frac{(y_{12} - s_y)^2}{z_2 - p_z} \pm \left[\frac{(y_{12} - s_y)^2}{2|s_z|} - \frac{\pi}{4\bar{k}} \right] \right\} \right)$$

(Here the upper sign corresponds to $s_z > 0$ and the lower sign to $s_z < 0$).

Using the results of the integrations, one obtains

$$\begin{aligned}
 \left\{ \hat{\Gamma}_S(x_{12}, y_{12}, z) \right\} &= \left(\frac{2}{\pi} \right)^{1/2} \frac{\bar{k}^3}{8} \iiint \exp \left[i\bar{k}(y_{12} - s_y)^2 \left(\frac{1}{z_2 - p_z} \pm \frac{1}{2|s_z|} \right) \right] \\
 &\frac{\sigma(x_{12}, y_{12}, s_z)}{(\bar{k}|s_z|)^{1/2}} \exp i \left(\bar{k}s_z \mp \frac{\pi}{4} \right) \left\{ \hat{\Gamma}_{j\Delta z}(x_{12}, s_y, s_z, p_z) \right\} ds_y ds_z dp_z,
 \end{aligned} \tag{B19}$$

which replaces Beran's Eq. (13) [B1].

It is possible to introduce a further simplification and carry out the integration over the s_y coordinate by making use of the smallness of the maximum eddy size measured in the y (the depth) direction. First, we notice that the minimum characteristic spread of $\left\{ \hat{\Gamma}_{j\Delta z} \right\}$ in the s_y direction is of order $(\ell_{zm}/\bar{k})^{1/2}$ (or $1/\bar{k}\theta_y$). Thus, if we require that this distance be much greater than ℓ_{ym} , the integration over s_y may be performed upon replacing the s_y argument in $\left\{ \hat{\Gamma}_{j\Delta z} \right\}$ by zero. In addition, s_y may be set equal to zero in the exponential terms if we have the somewhat stronger condition

$$\bar{k}\ell_{yM} \ll (\bar{k}\ell_{zm})^{1/2} \left(\frac{\ell_{zm}}{\ell_{zM}} \right)^{1/2} \tag{B20}$$

We note that we have already required that $(\bar{k}\ell_{zm}^2)/(\ell_{zM}) \gg 1$; see Eq. (B10). This same restriction also enables us to approximate

$$\exp [i\bar{k}y_{12}^2(z_2 - p_z)] \approx 1.$$

Carrying out the integration over s_y as a result of these three approximations leads to

$$\left\{ \hat{\Gamma}_S(x_{12}, y_{12}, z) \right\} = \left(\frac{2}{\pi} \right)^{1/2} \frac{\bar{k}^3}{8} \iint \exp \left[\pm i \left(\frac{\bar{k}y_{12}^2}{2|s_z|} - \frac{\pi}{4} \right) \right] \frac{\sigma_2(x_{12}, s_z)}{(\bar{k}|s_z|)^{1/2}} \exp(i\bar{k}s_z) \left\{ \hat{\Gamma}_{j\Delta z}(x_{12}, 0, s_z, p_z) \right\} ds_z dp_z. \quad (\text{B21})$$

where

$$\sigma_2(x_{12}, s_z) = \int_{-\infty}^{\infty} \sigma(x_{12}, s_y, s_z) ds_y.$$

In this appendix we accept the restriction given by Eq. (B20). We note, however, that a theory could be developed that would be valid for arbitrary $\bar{k}\ell_{yM}$ by retaining Eq. (B19). We would then find that $\left\{ \hat{\Gamma} \right\}$ is governed by an integral equation, the integration being over the variable s_y .

As a final observation we note that for narrow angle propagation we can write

$$\left\{ \hat{\Gamma}_{j\Delta z}(x_{12}, 0, s_z, p_z) \right\} \approx \exp(-iks_z) \left\{ \hat{\Gamma}_{j\Delta z}(x_{12}, 0, 0, 0) \right\}$$

for $|s_z| < \ell_m$ and $p_z < \Delta z$. This approximation allows us to carry out the integration over s_z and p_z , leading to

$$\left\{ \hat{\Gamma}_S(x_{12}, y_{12}, z) \right\} = \bar{\sigma}_2(x_{12}, y_{12}, z') \left\{ \hat{\Gamma}_{j\Delta z}(x_{12}, 0, j\Delta z) \right\} \quad (\text{B22})$$

where

$$\bar{\sigma}_2(x_{12}, y_{12}) = \left(\frac{2}{\pi} \right)^{1/2} \frac{\bar{k}^3}{4} \int_0^{\infty} \frac{\cos \left(\frac{\bar{k}y_{12}^2}{2|s_z|} - \frac{\pi}{4} \right)}{(\bar{k}|s_z|)^{1/2}} \sigma_2(x_{12}, s_z) ds_z \quad (\text{B23})$$

and $z' = z - j\Delta z$.

The condition for the validity of the single scattering approximation (which is a perturbation approximation) is readily seen to be

$$|\bar{\sigma}_2(x_{12}, y_{12})| \Delta z \ll 1. \quad (\text{B24})$$

The intensity of the scattered radiation is

$$\left\{ \hat{I}_S(z) \right\} = \left\{ \hat{\Gamma}_S(0, 0, z) \right\} = \bar{\sigma}_2(0, 0) \hat{I} z' \quad (\text{B25})$$

where I is the intensity of the initial radiation. For small angle scattering the intensity remains a constant independent of z . Thus, the intensity of the unscattered radiation must be

$$\left\{ \hat{I}_U(z) \right\} = (1 - \bar{\sigma}_2(0, 0) z') \hat{I}. \quad (\text{B26})$$

where $\left\{ \hat{I}_U(z) \right\}$ is the intensity of the unscattered radiation.

In this statistically homogeneous problem $\left\{ \hat{\Gamma}_{j\Delta z}(x_{12}, y_{12}, j\Delta z) \right\}$ may be derived by considering the superposition of an angular spectrum of plane waves. For small angle scattering the power in each plane wave is reduced by the same amount and thus

$$\left\{ \hat{\Gamma}_U(x_{12}, y_{12}, z) \right\} = \left\{ \hat{\Gamma}_{j\Delta z}(x_{12}, y_{12}, j\Delta z) \right\} [1 - \bar{\sigma}_2(0, 0) z'], \quad (\text{B27})$$

where $\left\{ \hat{\Gamma}_U(x_{12}, y_{12}, z) \right\}$ is the coherence function for the unscattered radiation.

The mutual coherence function is now given as the sum of the scattered and unscattered parts because these parts are uncorrelated. (The lack of correlation may be proven by a direct calculation.) Therefore, we write

$$\begin{aligned} \left\{ \hat{\Gamma}(x_{12}, y_{12}, z) \right\} &= \left\{ \hat{\Gamma}_{j\Delta z}(x_{12}, y_{12}, j\Delta z) \right\} [1 - \bar{\sigma}_2(0, 0) z'] \\ &+ \left\{ \hat{\Gamma}_{j\Delta z}(x_{12}, 0, j\Delta z) \right\} \bar{\sigma}_2(x_{12}, y_{12}) z', \end{aligned} \quad (\text{B28})$$

which leads to

$$\begin{aligned} \left\{ \hat{\Gamma}_{(j+1)\Delta z}(x_{12}, y_{12}, (j+1)\Delta z) \right\} &= \left\{ \hat{\Gamma}_{j\Delta z}(x_{12}, y_{12}, j\Delta z) \right\} (1 - \bar{\sigma}_2(0, 0)\Delta z) \\ &+ \left\{ \hat{\Gamma}_{j\Delta z}(x_{12}, 0, j\Delta z) \right\} \bar{\sigma}_2(x_{12}, y_{12})\Delta z. \end{aligned} \quad (\text{B29})$$

The difference equation can be approximated by the following differential equation:

$$\begin{aligned} \frac{\partial \left\{ \hat{\Gamma}(x_{12}, y_{12}, z) \right\}}{\partial z} &= - \left\{ \hat{\Gamma}(x_{12}, y_{12}, z) \right\} \bar{\sigma}_2(0, 0) \\ &+ \left\{ \hat{\Gamma}(x_{12}, 0, z) \right\} \bar{\sigma}_2(x_{12}, y_{12}). \end{aligned} \quad (\text{B30})$$

We note that Eq. (B30) follows exactly from Eq. (B29) in the limit of $\Delta z \rightarrow 0$. In our treatment, however, this step must be taken as an approximation because in deriving Eq. (B29) we introduced the restriction that $\Delta z \gg \ell_{zM}$. The nature of the approximation is similar to that used in continuum fluid mechanics where we allow the elemental volume size ΔV to approach zero even though it must satisfy the restriction $(\Delta V)^{1/3} \gg \ell_p$, where ℓ_p is the molecular mean free path.

The solution of Eq. (B27) for an initial plane wave is

$$\left\{ \hat{\Gamma}(x_{12}, y_{12}, z) \right\} = \hat{I} \left(\frac{\bar{\sigma}_2(x_{12}, y_{12})}{\bar{\sigma}_2(x_{12}, 0)} \exp \left\{ -[\bar{\sigma}_2(0, 0) - \bar{\sigma}_2(x_{12}, 0)]z \right\} + \left[1 - \frac{\bar{\sigma}_2(x_{12}, y_{12})}{\bar{\sigma}_2(x_{12}, 0)} \right] \exp [-\bar{\sigma}_2(0, 0)z] \right). \quad (\text{B31})$$

To study the coherence function $\left\{ \hat{\Gamma}(x_{12}, y_{12}, z) \right\}$ we thus only require a knowledge of the function $\bar{\sigma}_2(x_{12}, y_{12})$.

Two special cases of Eq. (B31) are of interest. They are

$$\left\{ \hat{\Gamma}(x_{12}, 0, z) \right\} = \hat{I} \exp \left\{ -[\bar{\sigma}_2(0, 0) - \bar{\sigma}_2(x_{12}, 0)]z \right\}, \quad (2)$$

and

$$\left\{ \hat{\Gamma}(0, y_{12}, z) \right\} = \hat{I} \left\{ \frac{\bar{\sigma}_2(0, y_{12})}{\bar{\sigma}_2(0, 0)} + \left[1 - \frac{\bar{\sigma}_2(0, y_{12})}{\bar{\sigma}_2(0, 0)} \right] \exp [-\bar{\sigma}_2(0, 0)z] \right\}. \quad (3)$$

The function $\left\{ \hat{\Gamma}(x_{12}, 0, z) \right\}$, for example, allows us to determine the horizontal resolution of an aperture system, whereas $\left\{ \hat{\Gamma}(0, y_{12}, z) \right\}$ allows us to determine the vertical resolution. As $z \rightarrow \infty$, Eq. (3) approaches the simple limit

$$\left\{ \hat{\Gamma}(0, y_{12}, z \rightarrow \infty) \right\} = \hat{I} \frac{\bar{\sigma}_2(0, y_{12})}{\bar{\sigma}_2(0, 0)}. \quad (\text{B33})$$

We synopsize here the conditions to be satisfied for the validity of Eq. (B30):

$$(i) \quad \bar{k} \ell_{yM} \ll (\bar{k} \ell_{zm})^{1/2} \left(\frac{\ell_{zm}}{\ell_{zM}} \right)^{1/2} \quad (\text{B34})$$

$$(ii) \quad \bar{\sigma}_2(0, 0) \Delta z \ll 1$$

where Δz is a distance that satisfies the inequalities

$$\frac{\ell_{zM}^2}{\ell_{zm}} \ll \Delta z \ll \frac{1}{\bar{k} \theta_x^2}. \quad (\text{B35})$$

REFERENCE

B1. M. J. Beran, J. Opt. Soc. Amer. **S6**, 1475 (1966).

Appendix C

A NUMERICAL STUDY

We present here the results of a numerical study of Eq. (12) in which we introduce the most refined estimate of $\Phi_1(p)$ that can be supported by reported data and the more generally accepted theoretical arguments. These results are then compared with those obtained by making use of Eqs. (15) and (16), which are based on a -2 power law for $\Phi_1(p)$.

It is generally accepted that the larger scale temperature fluctuations arise because of the presence of randomly phased internal waves and the smaller scale fluctuations because of ocean turbulence. The fact that two distinctly different mechanisms may be acting suggests that the temperature fluctuation spectrum may have a different functional form for large values of $1/p$ corresponding to large size-scale fluctuations than it does for small values of $1/p$ corresponding to small size-scale fluctuations. There appears to be less agreement on the hypothesis that associated with randomly phased internal wave fields is a uniquely defined functional form for $\Phi_1(p)$ to which can be assigned some degree of universality. A definitive answer to this question must await the development of a comprehensive and experimentally verified theory of internal waves. At present the strongest evidence would suggest that internal waves will give rise to a spectrum that behaves as p^{-2} over at least a range of wave numbers. Phillips [C1] presents an argument supporting a low wave number p^{-2} behavior and a higher wave number p^{-3} behavior. Also, the sheet and layer model of Phillips [C1] results in a -2 law. Similarly, experimental data support a -2 law for size scales of the order of a few thousands of meters. See, for example, Charnock [C2] and McKean and Ewart [C3]. We might note that the data of Charnock also appear to support the presence of a -1 region at the largest size scale observations. These data are extremely sketchy, however, and are not included in our estimate of $\Phi_1(p)$. We note that the description of the scattering phenomenon constructed in the section on the dependence of Γ on the temperature microstructure suggests that any very large scale -1 behavior would be significant only for very large separation distances; i.e., of the order of several tens of thousands of meters. For small size scale ocean turbulence, the familiar Kolmogorov spectrum (i.e., $p^{-5/3}$ law) might be expected. A $-5/3$ region has been observed. See, for example, Grant, Stewart and Moilliet [C4] and Moseley and Del Balzo [C5]. The relatively larger size scale ocean turbulence can be expected to vary as p^{-3} because of the influence of buoyancy forces. The data of Moseley and Del Balzo [C5] indicate the presence of a -3 transition region. Introducing each of these factors into our estimate of $\Phi_1(p)$, we achieve the composite spectrum sketched in Fig. C1.

The composite spectrum contains six environmental parameters; i.e., the low and high wave number cutoffs, the transition wave number, and the coefficients A_2^2 , B^2 , and C^2 . In our numerical study we made estimates of these parameters and, using these, evaluated the integral in Eq. (10).

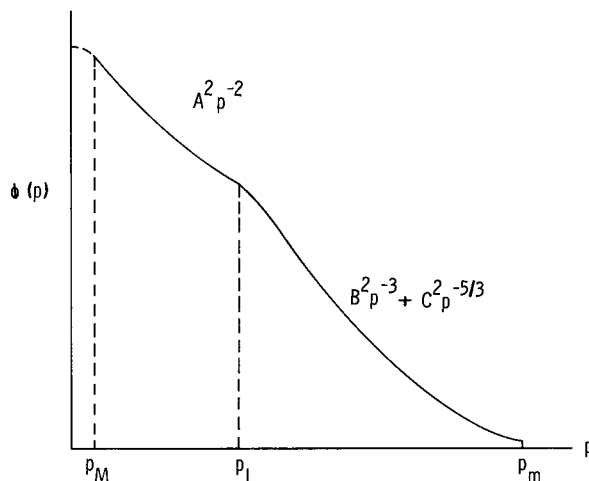


Fig. C1 — Functional form of fluctuation power spectrum used in numerical studies

$$\bar{\sigma}(0, 0) - \bar{\sigma}_2(x_{12}, 0) = \frac{\bar{k} \ell_{yM} x_{12}^{1/2}}{2^{3/2}} \int_0^\infty F(px_{12}) \Phi_1(p) dp \quad (10)$$

where

$$F(px_{12}) = \frac{1}{(px_{12})^{1/2}} - \frac{\Gamma(4)}{2^{3/2}} (px_{12})^{1/4} J_{-3/4}(px_{12}).$$

The values of A_2^2 and p_M were then used in

$$\begin{aligned} \bar{\sigma}_2(0, 0) - \bar{\sigma}_2(x_{12}, 0) &= 0.641 A_2^2 \bar{k}^{5/2} \ell_{yM} \\ &\times \left[\frac{1.216}{p_M^{3/2}} - 1.19 \left(\frac{x_{12}}{p_M} \right)^{3/4} K_{3/4}(p_M x_{12}) \right], \end{aligned} \quad (15)$$

A_2^2 was used in

$$\bar{\sigma}_2(0, 0) - \bar{\sigma}_2(x_{12}, 0) = 1.1 A_2^2 \ell_{yM} \bar{k}^{5/2} x_{12}^{3/2}, \quad (16)$$

and the desired comparisons were made.

We now consider the reasoning that led to the choice of values for the six environmental parameters. Summers and Emery [C6] have reported data of internal waves with approximately semidiurnal periods propagating in deep water with a speed of approximately

7 knots. This corresponds to a wavelength of the order of 100 km. Based on this observation we shall take $p_M^{-1} = 10^5/2\pi$ m in our numerical studies and later will discuss the relative insensitivity of this choice for cases of interest. The transition wave number p_1 is not expected to have a uniquely prescribed value. Rather, it represents a transition region, presumably small, between the $A_2^2 p^{-2}$ region and the $B^2 p^{-3} + C^2 p^{-5/3}$ region. A sharply defined transition wave number may be imagined by extending the $A_2^2 p^{-2}$ and the $B^2 p^{-3} + C^2 p^{-5/3}$ regions until they intercept. Thus, p_1 is, in fact, defined by the measured values of A_2^2 , B^2 , and C^2 and is not, itself, a directly measurable quantity. Of course, for spectra in which a sharply defined transition region between the $A_2^2 p^{-2}$ and the $B^2 p^{-3} + C^2 p^{-5/3}$ regions is clearly visible one does have a direct way to estimate p_1 . Unfortunately, there are no published data in which estimates of A_2^2 , B^2 , and C^2 have all been obtained. Usually, sea data of the temperature spectrum concentrate on either the larger scale structure or the smaller scale structure. Thus, we are required to rely on either large scale data, which give us estimates of A_2^2 , and extrapolate these to the smaller scale region, or vice versa. In our program we relied on the data of Moseley and Del Balzo [C5], which provide estimates of B^2 and C^2 . This leaves us with the task of extrapolating these data to the larger size scale portion of the spectrum. The extrapolation is accomplished by making estimates of the location of the transition region, i.e., of p_1 . The smallest estimate chosen for p_1 was $2\pi/1,500$ m⁻¹. This wave number corresponds to a size scale of 1,500 m. It would appear to be generally accepted that a size scale of this magnitude will certainly be larger than that at which the transition will occur. Additional estimates chosen for p_1 correspond to size scales of the order of 1,000 and 500 m. Estimates of p_1 corresponding to smaller size scales were not chosen for two reasons: (a) the data of Moseley and Del Balzo, which included size scales of the order of several hundred meters, did not show the transition region, and (b) the sensitivity of the results of interest to the actual value of p_1 was seen to be not very great if p_1 is of the order of $2\pi/500$ m⁻¹, or larger. The data of Moseley and Del Balzo extend to very large values of p and indicate the presence of turbulent eddies containing measurable amounts of energy, which are of the order of meters or less in spatial extent. However, we have argued in the section on the dependence of $\{\Gamma\}$ on the temperature microstructure, the acoustic signal coherence will depend on these small eddies only for separation distances of the same order of size. Because the present work is devoted to long ranges and low frequencies, we will allow p_m to be infinitely large in our numerical studies.

As previously stated, we relied on the data of Moseley and Del Balzo to make estimates of B^2 and C^2 . Three sets of values were selected that encompass the range of values observed in their data. The specific values chosen are given in Table C1. (We have

Table C1
Parameters Chosen for Numerical Study*

Conditions	$B^2(m^{-2})$	$C^2(m^{-2/3})$
Weak fluctuations	4×10^{-14}	5×10^{-12}
Moderate fluctuations	3×10^{-13}	2×10^{-11}
Strong fluctuations	3.3×10^{-12}	2×10^{-10}

*After Ref. C5.

introduced the scale factors required to change the Moseley and Del Balzo temperature data into refractive index data and to compensate for differences in the definitions of the spectrum.) The terminology of “strong”, “moderate”, and “weak” is to be interpreted in a relative sense in that they only denote the largest, a middle, and the smallest of the values encountered during the same experiment performed over a relatively short time interval at essentially the same location. (The differing fluctuation spectra observed were obtained from tow runs at different depths.)

In Fig. C2 we present the dependence of the calculated A_2^2 values as functions of p_1 for the three fluctuation conditions denoted as strong, moderate, and weak. These values can be compared with those reported by Mc Kean and Ewart [C3], which range between 10^{-11} and 5×10^{-9} . (Again, we have introduced the requisite scale factor.) Although the McKean and Ewart data analysis is based on a -2 power law curve fit for much higher wave numbers than envisioned by our extrapolation, the agreement between the values is striking.

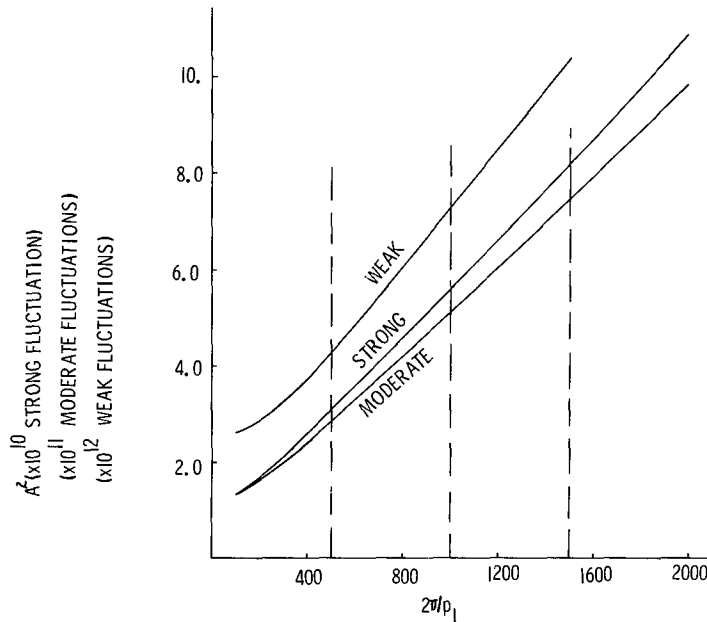


Fig. C2 — Dependence of extrapolated A_2^2 values on p_1 .
 (Strong: $B = 3.3 \times 10^{-12}$, $C = 2 \times 10^{-10}$; moderate:
 $B = 3 \times 10^{-13}$, $C = 2 \times 10^{-11}$; weak: $B = 4 \times 10^{-14}$,
 $C = 5 \times 10^{-12}$)

Figures C3 through C5 illustrate the dependence of $L(x_{12})x_{12}^{1/2}$ where $L(x_{12})$ is the integral in Eq. (10), for the nine spectra described in this appendix. Also drawn are line graphs of the values given for $L(x_{12})x_{12}^{1/2}$ by Eqs. (15) and (16). We note that the dependence of the latter expressions on p_1 is via the coefficient A_2^2 . This dependence is, therefore, an apparent dependence arising from the manner in which A_2^2 was obtained.

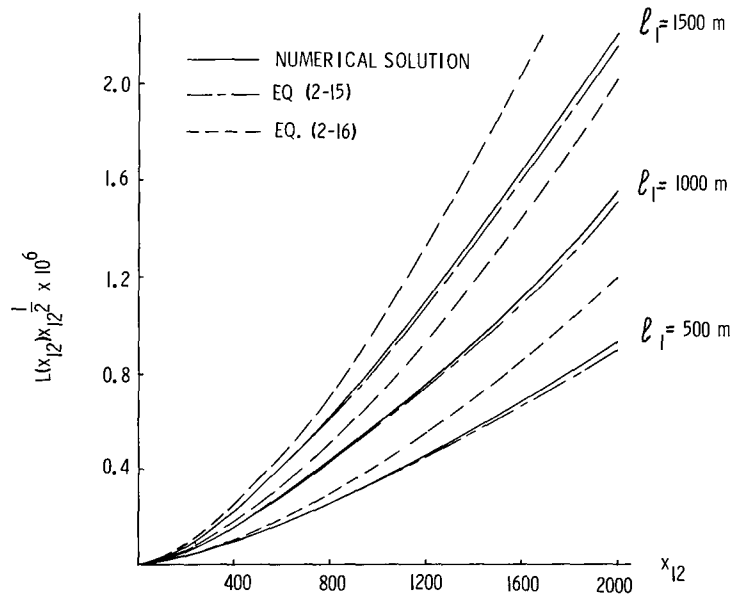


Fig. C3 — Dependence of exponent function on separation distance for weak fluctuations. $p_M = 2\pi/10^5 \text{ m}^{-1}$; $\ell_1 = 2\pi/p_1$.

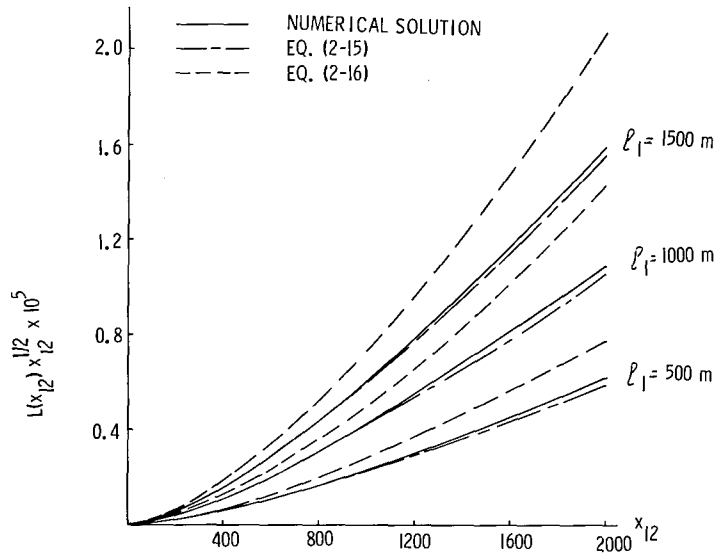


Fig. C4 — Dependence of exponent function on separation distance for moderate fluctuations. $p_M = 2\pi/10^5 \text{ m}^{-1}$; $\ell_1 = 2\pi/p_1$.

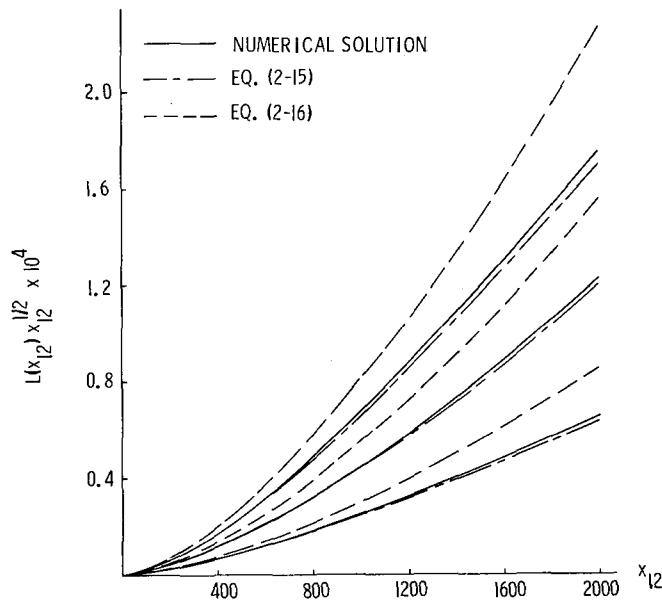


Fig. C5 — Dependence of exponent function on separation distance for strong fluctuations. $p_M = 2\pi/10^5 m^{-1}$; $q_1 = 2\pi/p_1$.

The most important conclusion to be drawn from these curves is the excellent agreement that can be obtained if we replace the composite spectrum with a more easily handled -2 power-law spectrum. A more significant error results from expanding and truncating the Bessel function, which is required to obtain Eq. (16) from Eq. (15), even though this error is still not very significant. For shorter separation distances the percentage difference in the values given by the numerical solution from those given by Eqs. (15) and (16) increases. This increase cannot be discerned from the line graphs, however, because the actual values are small for the scale of the line graphs.

In Fig. C6 we show the results of an investigation of the sensitivity of the results to the value chosen for p_M . The conclusion to be drawn from this figure is that the results are insensitive to the actual value of p_M as long as the largest size scale is of the order of 100 km. The sensitivity is greatly increased, however, if the largest size scale is of the order of 10 km.

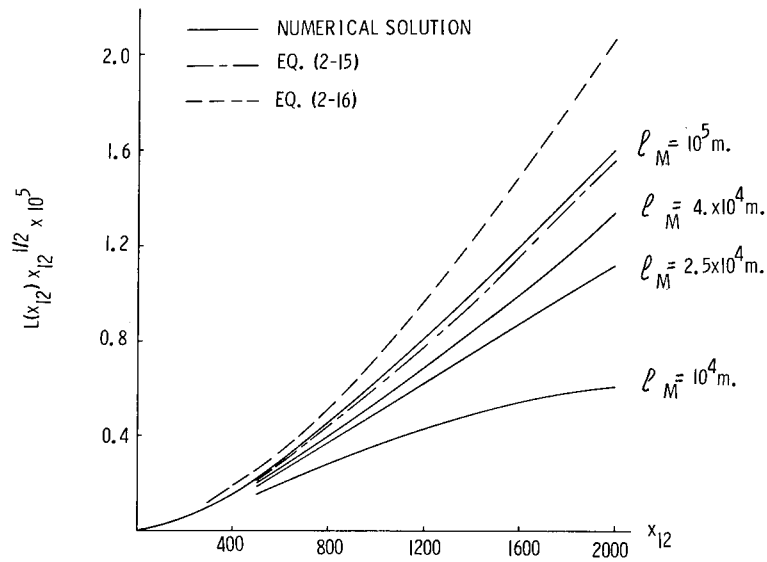


Fig. C6 — Dependence of exponent function on separation distance for moderate fluctuations. $p_1 = 2\pi/1,500 \text{ m}^{-1}$; $\ell_M = 2\pi/p_M$.

REFERENCES

- C1. O. M. Phillips, *The Dynamics of the Upper Ocean*, Cambridge University Press, London, 1969.
- C2. H. Charnock, *Proc. 2d U. S. Navy Symp. Military Oceanogr.*, 1965, p. 175.
- C3. R. S. McKean and T. E. Ewart, *J. Phys. Oceanogr.* **4**, No. 2, 191 (1974).
- C4. H. L. Grant, R. W. Stewart, and A. Moilliet, *J. Fluid Mech.* **12**, 241 (1962).
- C5. W. B. Moseley and D. R. Del Balzo, "Oceanic Horizontal Random Temperature Structure," *NRL Report 7673*, July 1974.
- C6. H. L. Summers and K. O. Emery, *J. Geophys. Res.* **68**, 827 (1963).

Appendix D

EFFECTS OF NONHOMOGENEITY, REFLECTION, AND SOURCE SIZE

In our analysis of the temperature microstructure effects on array size we have assumed that we could arrive at the correct order of magnitude by considering the propagation of a plane wave through a statistically homogeneous medium. In the ocean the acoustic radiation will pass through regions with mean temperature gradients and variable statistical properties, and be reflected at both the ocean surface and bottom. In addition, we shall be dealing with a finite source size. The purpose of this section is to show that the additional effects of mean temperature gradient, statistical inhomogeneities, and finite source size do not change the order of magnitude of our results. The question of surface reflection may require special attention.

As in the main body of the report, we restrict attention to the coherence function for separation distances taken along the x axis. It is this function that determines azimuthal angular spread. The complexity of the problem necessitates our approaching it in a two-step procedure. Thus, we first consider only an average of the coherence function taken over the vertical direction and discuss, in turn, the effects of a mean sound-speed profile, of superimposed inhomogeneities in the statistics of the fluctuating refractive index field, and of a finite source. Next we discuss, in the light of the previous discussion, the effects of these same inhomogeneities on the angular spread that would be measured by a horizontal line array positioned at a fixed depth. Finally, we consider the effects of surface reflections.

To consider this problem, it is first necessary to develop the differential equation that governs the mutual coherence when diffraction, refraction, and scattering are all important. This formulation is quite easily accomplished by considering the incremental derivation procedure of Appendix B. The fundamental assumption to be made in deriving the differential equation is that for propagation distances of the order of Δz , the effects of diffraction, refraction, and scattering are all uncoupled. Thus, we only need add a diffraction term and a refraction term to Eq. (B30). Recalling that a condition for the validity of the theory is that the angular spectral representation of the beam be narrow, one can show* that the appropriate diffraction term is

$$\frac{i}{2\langle k \rangle} \left(\nabla_{\mathbf{x}_{T1}}^2 - \nabla_{\mathbf{x}_{T2}}^2 \right) \left\{ \hat{\Gamma}(\mathbf{x}_{T1}, \mathbf{x}_{T2}, z) \right\}$$

where $\langle k \rangle$ is an average of $k(y)$ taken over the width of the beam and \mathbf{x}_{T1} and \mathbf{x}_{T2} are the transverse parts of position vectors \mathbf{x}_1 and \mathbf{x}_2 , respectively.

The appropriate refraction term is

$$i[\bar{k}(y_1) - \bar{k}(y_2)] \left\{ \hat{\Gamma}(\mathbf{x}_{T1}, \mathbf{x}_{T2}, z) \right\} .$$

*M. J. Beran, *J. Opt. Soc. Amer.* **60**, 518 (1970).

Thus the equation governing the mutual coherence function is written

$$\begin{aligned}
 \frac{\partial}{\partial z} \left\{ \hat{\Gamma}(\mathbf{x}_{T1}, \mathbf{x}_{T2}, z) \right\} &= - \langle \bar{k}^2 \rangle \bar{\sigma}_2(0) \left\{ \hat{\Gamma}(\mathbf{x}_{T1}, \mathbf{x}_{T2}, z) \right\} \\
 &+ \langle \bar{k}^2 \rangle \bar{\sigma}_2(x_{12}, y_{12}) \left\{ \hat{\Gamma}(x_1, x_2, \frac{y_1+y_2}{2}, 0, z) \right\} \\
 &+ \frac{i}{2\langle \bar{k} \rangle} (\nabla_{\mathbf{x}_{T1}}^2 - \nabla_{\mathbf{x}_{T2}}^2) \left\{ \hat{\Gamma}(\mathbf{x}_{T1}, \mathbf{x}_{T2}, z) \right\} \\
 &+ i[\bar{k}(y_1) - \bar{k}(y_2)] \left\{ \hat{\Gamma}(\mathbf{x}_{T1}, \mathbf{x}_{T2}, z) \right\}.
 \end{aligned} \tag{D1}$$

The operators $\nabla_{\mathbf{x}_{T1}}^2$ and $\nabla_{\mathbf{x}_{T2}}^2$ depend on the transverse coordinates x and y . The coherence function depends on the variables z , x_1 , x_2 , y_1 , and y_2 . The equation simplifies if we transform to the coordinates

$$\begin{aligned}
 p_x &= \frac{1}{2}(x_1+x_2), \quad p_y = \frac{1}{2}(y_1+y_2), \\
 s_x &= x_1 - x_2, \quad s_y = y_1 - y_2.
 \end{aligned} \tag{D2}$$

In terms of these coordinates, Eq. (D1) becomes

$$\begin{aligned}
 \frac{\partial}{\partial z} \left\{ \hat{\Gamma} \right\} &= - \langle \bar{k}^2 \rangle \bar{\sigma}_2(0) \left\{ \hat{\Gamma} \right\} + \langle \bar{k}^2 \rangle \bar{\sigma}_2(\mathbf{s}) \left\{ \hat{\Gamma}(s_x, p_x, 0, p_y, z) \right\} \\
 &+ \frac{i}{\langle \bar{k} \rangle} \left(\frac{\partial}{\partial p_x} \frac{\partial}{\partial s_x} + \frac{\partial}{\partial p_y} \frac{\partial}{\partial s_y} \right) \left\{ \hat{\Gamma} \right\} \\
 &+ i[\bar{k}(p_y+s_{y2}) - \bar{k}(p_y-s_{y2})] \left\{ \hat{\Gamma} \right\}.
 \end{aligned} \tag{D3}$$

Equation (D3) governs the plane wave solutions we have previously considered and also propagation from a finite source. In treating the effect of $\bar{k}(y)$ we shall consider the radiation to be confined to $0 \leq p_y \leq H$ (where $z = 0$ is the mean ocean bottom and $z = H$ the mean ocean surface) rather than assume an initial plane wave.

We shall first focus our attention on the average quantity

$$\left\langle \left\{ \hat{\Gamma}(s_x, s_y, p_x, z) \right\} \right\rangle = \frac{1}{H} \int_0^H \left\{ \hat{\Gamma}(s_x, s_y, p_x, p_y, z) \right\} dp_y \tag{D4}$$

for $s_y = 0$. By integrating over p_y and dividing by H we have the average coherence of radiation in the y direction. If we then set s_y we find the average intensity in the y direction. Therefore $\langle \Gamma(s_x, 0, p_x, z) \rangle$ represents the effects of only horizontal scattering.

Integrating Eq. (D3) from p_y equal 0 to H and dividing by H yields

$$\begin{aligned} \frac{\partial}{\partial z} \langle \Gamma \rangle &= - \langle \bar{k}^2 \rangle \bar{\sigma}_2(0) \langle \Gamma \rangle + \langle \bar{k}^2 \rangle \bar{\sigma}_2(s) \frac{1}{H} \int_0^H \Gamma(s_x, p_x, 0, p_y, z) dp_y \\ &+ \frac{i}{\langle \bar{k} \rangle} \frac{\partial}{\partial s_x} \frac{\partial}{\partial p_x} \langle \Gamma \rangle + \frac{\partial}{\partial s_y} \frac{1}{H} \left(\langle \Gamma \rangle_{p_y=H} - \langle \Gamma \rangle_{p_y=0} \right) \\ &+ i \frac{1}{H} \int_0^H \left[\bar{k} \left(p_y + \frac{s_y}{2} \right) - \bar{k} \left(p_y - \frac{s_y}{2} \right) \right] \Gamma dp_y \end{aligned} \quad (D5)$$

Setting $s_y = 0$ then gives

$$\begin{aligned} \frac{\partial}{\partial z} \langle \Gamma \rangle &= \langle \bar{k}^2 \rangle [\bar{\sigma}_2(s_x) - \bar{\sigma}_2(0)] \langle \Gamma \rangle \\ &+ \frac{i}{\langle \bar{k} \rangle} \frac{\partial}{\partial s_x} \frac{\partial}{\partial p_x} \langle \Gamma \rangle + \frac{\partial}{\partial s_y} \frac{1}{H} \left(\langle \Gamma \rangle_{p_1=H} - \langle \Gamma \rangle_{p_y=0} \right) \end{aligned} \quad (D6)$$

where $s_y = 0$ in all terms is to be understood.

The last term in the right hand side of Eq. (D6) may be set equal to zero since H is large compared to any characteristic coherence length. That this is valid can be seen by integrating the equation from $0-\epsilon$ to $H+\epsilon$ and taking the limit $\epsilon \rightarrow 0$. Outside the interval $0 \leq p_y \leq H$, $\Gamma = 0$. The equation governing $\langle \Gamma \rangle$ is then

$$\frac{\partial}{\partial z} \langle \Gamma \rangle = \langle \bar{k}^2 \rangle [\sigma_2(s_x) - \bar{\sigma}_2(0)] \langle \Gamma \rangle + \frac{i}{\langle \bar{k} \rangle} \frac{\partial}{\partial p_x} \frac{\partial}{\partial s_x} \langle \Gamma \rangle \quad (D7)$$

From Eq. (D7) we see that the variation in mean index of refraction (as given by $\bar{k}(y)$) has no effect on the average scattering in the horizontal direction.

We next turn to the question of statistical inhomogeneities in the fluctuation field. The inhomogeneity is exhibited by making σ_2 an explicit function of p_y . Examination of the assumptions made in the derivation of Eq. (D1) shows that, in the statistically inhomogeneous case, Eqs. (D1) and (D3) are still valid if $\sigma_2(0)$ and $\sigma_2(s)$ are replaced by $\sigma_2(0, p_y)$ and $\sigma_2(s, p_y)$, respectively. Manipulations similar to those that led to Eq. (D7) now yield

$$\begin{aligned} \frac{\partial}{\partial z} \langle \hat{\Gamma} \rangle &= \frac{\langle \bar{k}_z \rangle}{H} \int_0^H [\bar{\sigma}_2(s_x, p_y) - \bar{\sigma}_2(0, p_y)] \left\{ \hat{\Gamma}(s_x, p_x, 0, p_y, z) \right\} dp_y \\ &+ \frac{i}{\langle \bar{k} \rangle} \frac{\partial}{\partial p_x} \frac{\partial}{\partial s_x} \langle \hat{\Gamma} \rangle. \end{aligned} \quad (\text{D8})$$

Eq. (D8) is not a determinate equation governing $\langle \hat{\Gamma} \rangle$. When σ_2 is a function of p_y , the amount of horizontal scattering depends upon the height at which the scattering occurs, and it is not possible to remove the $\bar{\sigma}_2(s_x, p_y) - \bar{\sigma}_2(0, p_y)$ term from under the integral.

We note that formally we can express the integral in Eq. (D8) in the form

$$\begin{aligned} \frac{1}{H} \int_0^H [\bar{\sigma}_2(s_x, p_y) - \bar{\sigma}_2(0, p_y)] \left\{ \hat{\Gamma}(s_x, p_x, 0, p_y, z) \right\} dp_y \\ = \langle \bar{\sigma}_2(s_x) - \bar{\sigma}_2(0) \rangle_{W(z)} \langle \hat{\Gamma}(s_x, p_x, 0, z) \rangle \end{aligned} \quad (\text{D9})$$

where $\langle \bar{\sigma}_2(s_x) - \bar{\sigma}_2(0) \rangle_{W(z)}$ is interpreted as a weighted average of the $\bar{\sigma}_2$ terms. The weighted average is shown to depend on range z because the weighting function depends on range. This formal expression, as such, does not gain anything because it only represents a prescription for evaluating the required average of the $\bar{\sigma}_2$ terms after one has solved the problem for $\left\{ \hat{\Gamma}(s_x, p_x, 0, p_y, z) \right\}$. It could be useful, on the other hand, for particular situations in which it is possible to estimate the averaged $\bar{\sigma}_2$ terms, a priori.

To motivate this type of reasoning, we might note that the dependence of $\left\{ \hat{\Gamma}(s_x, p_x, 0, p_y, z) \right\}$ on p_y is a measure of the radiation intensity at the height determined by p_y . (That is,

$$\left\{ \hat{I}_y(p_y, z) \right\} = \int_{-\infty}^{\infty} \left\{ \hat{\Gamma}(0, p_x, 0, p_y, z) \right\} dp_x$$

is equal to the total radiation intensity at p_y .) Thus, to first order, we might attempt to replace $\left\{ \hat{\Gamma}(s_x, p_x, 0, p_y, z) \right\}$ as a weighting function by $\left\{ \hat{I}_y(p_y, z) \right\}$. This leads to

$$\langle \bar{\sigma}_2(s_x) - \bar{\sigma}_2(0) \rangle_{W(z)} \equiv \frac{\int_0^H \left\{ \hat{I}_y(p_y, z) \right\} [\bar{\sigma}_2(s_x, p_y) - \bar{\sigma}_2(0, p_y)] dp_y}{\int_0^H \left\{ \hat{I}_y(p_y, z) \right\} dp_y} \quad (\text{D10})$$

as an approximation for the averaged $\bar{\sigma}_2$ terms. We could note that the approximation expressed by Eq. (D10) does not of itself lead to a determinate problem because $\left\{ \hat{I}_y(p_y, z) \right\}$ is, of course, unknown until the whole problem is solved. Now, however, we are in a

position to make an intelligent guess by solving for $\{\hat{I}_y\}$ in the absence of scattering (i.e., considering only refraction and diffraction effects) or by first solving the whole problem, assuming that

$$\langle \bar{\sigma}_2(s_x) - \bar{\sigma}_2(0) \rangle_{W(z)} = \frac{1}{H} \int_0^H [\bar{\sigma}_2(s_x, p_y) - \bar{\sigma}_2(0, p_y)] dp_y. \quad (D11)$$

Equation (D10) and the intelligent guess for $\{\hat{I}_y\}$ do make the problem on $\langle \{\hat{\Gamma}(s_x, p_x, z)\} \rangle$ determinate.

The weakness in this procedure is Eq. (D10). In general,

$$\left\{ \hat{\Gamma}(s_x, p_x, 0, p_y, z) \right\} \neq \frac{\left\{ \hat{I}_y(p_y, z) \right\} \left\{ \hat{\Gamma}(s_x, p_x, z) \right\}}{\int_0^H \left\{ \hat{I}_y(p_y, z) \right\} dp_y} \quad (D12)$$

as is required for Eq. (D10) to be exact. That is, the amount of scattering that occurs at the position located by p_x, p_y depends on the specific intensity and angular distribution at this point and not just on the average intensity at the height p_y . If the radiation followed a single path, then Eq. (D10) would be an excellent approximation. If, however, the radiation followed two or more paths, and the fluctuations encountered over the differing multipaths were statistically different, Eq. (D12) would be expected to be in serious error. For the long ranges of interest to us, it is felt that the latter situation is unlikely and that the many multipaths present will all traverse the same range of depths.

Equation (D11) would be expected to be reasonable only in the absence of any sound trapping. For propagation in the sound channel, it would be more reasonable to replace Eq. (D11) with an average taken over the depth of the sound channel.

We will assume that the appropriate equation for $\langle \{\hat{\Gamma}\} \rangle$ is

$$\frac{\partial}{\partial z} \langle \{\hat{\Gamma}\} \rangle = \langle \bar{k}^2 \rangle \langle \bar{\sigma}_2(s_x) - \bar{\sigma}_2(0) \rangle_{W(z)} \langle \{\hat{\Gamma}\} \rangle + \frac{i}{\langle \bar{k} \rangle} \frac{\partial}{\partial p_x} \frac{\partial}{\partial s_x} \langle \{\hat{\Gamma}\} \rangle \quad (D13)$$

where $\langle \bar{\sigma}_2(s_x) - \bar{\sigma}_2(0) \rangle_{W(z)}$ is given by Eq. (D10). For long paths we expect this term to be almost independent of z , and in any case it may be considered to vary slowly with z .

This effect of finite source size is given by the derivative term on the right hand side of Eq. (D13). Equation (D13), except for a change in the definition of $\langle \bar{\sigma}_2 \rangle$, is identical to the equation one obtains when $\lambda \ll l_{Vm}$ in addition to the condition $\lambda \ll l_{Hm}$. In this case many solutions are available for finite sources, and it is known that, to within a constant of order unity (say 1 to 3), the characteristic scattering angle is the same as the plane wave case. Thus to arrive at the order of magnitude, we may use the plane wave results to estimate resolution from finite sources. Similarly we may assume that, also in the case when $\lambda \geq l_{VM}$, the plane wave solution is adequate, for obtaining the order of magnitude, to estimate the resolution when the source is finite.

A final question of the effects of nonhomogeneity and of finite source size concerns the relation between $\langle \hat{\Gamma}(s_x, p_x, z) \rangle$ and the coherence function that is measured if the detector is a linear array at fixed height $p_y = h$; i.e., if $\langle \hat{\Gamma}(s_x, p_x, 0, h, z) \rangle$ is measured. In general, $\langle \hat{\Gamma}(s_x, p_x, z) \rangle$ and $\langle \hat{\Gamma}(s_x, p_x, 0, h, z) \rangle$ may be quite different, but, if we consider long path lengths and if $p_y = h$ is a height such that $\langle \hat{I}_y(h, z) \rangle$ is large, then we may expect the two functions to be very similar in order of magnitude. If, for example, a sound channel is present, we would place the detector at a height within the channel. We shall assume that the detector height is not chosen at random but at a height such that $\langle \hat{I}_y(h, z) \rangle$ is close to the average intensity:

$$\langle \hat{I} \rangle = \int_{-\infty}^{\infty} \langle \hat{\Gamma}(0, p_x, z) \rangle dp_x.$$

In summary, we have shown that to obtain results that are correct in order of magnitude when (a) there is a mean index-of-refraction gradient, (b) the statistics of the index-of-refraction field are inhomogeneous in the vertical direction, and (c) the source is finite, it is sufficient to use the equation

$$\frac{\partial \langle \hat{\Gamma} \rangle}{\partial z} = \langle \bar{k}^2 \rangle \langle \bar{\sigma}_2(s_x) - \bar{\sigma}_2(0) \rangle_{W(z)} \langle \hat{\Gamma} \rangle + \frac{i}{\langle \bar{k} \rangle} \frac{\partial}{\partial p_x} \frac{\partial}{\partial s_x} \langle \hat{\Gamma} \rangle$$

where $\langle \bar{\sigma}_2(s_x) - \bar{\sigma}_2(0) \rangle_{W(z)}$ is given by Eq. (D10) and may be taken to be independent of z when z is large.

The effect that may be more critical is that of scattering from the ocean surface and bottom. To the extent that the ocean surface or bottom may be considered to be a plane horizontal surface, these surfaces do not affect the results obtained. In this case the radiation simply reflects, with the magnitude of the angular spectrum unchanged. When the surfaces are not planes, the scattering over the rough surface must be calculated based on knowledge of the surface characteristics. There is a large amount of literature devoted to this subject, but it is beyond the scope of the present work. The results we have obtained do put a lower bound on the scattering, however, because the effects of internal and surface scattering should be additive.

Appendix E

BACKGROUND DISCUSSION OF APERTURE PROBLEM

The study of the statistical properties of pressure fields and electromagnetic fields propagating in random media has been an active research area since the 1940's. Principal contributions have appeared in both the Western and Soviet literature. In this section we shall briefly survey the developments in the past 25 years that are most closely related to the study presented in this report.

The Soviet literature is most easily surveyed because there are three books that bring us abreast of developments through about 1970 [E1-E5]. Chernov [E1] and Tatarski [E2] are widely quoted in the Western literature and give fairly complete references to works in both Soviet and Western literature before about 1960. In these books the statistical problem is clearly formulated in terms of phase and amplitude fluctuations. Calculations are made for the phase and amplitude two-point correlation functions in terms of the statistical properties of the index-of-refraction field. In Chernov's book [E1] the index-of-refraction field is represented by two-point correlation functions with a single length parameter, but in Tatarski's book [E2] the Kolmogorov spectrum is used. The principal limitation of these two books is that the solutions are essentially single scatter solutions despite the claims made for the validity of the Rytov approximation in the multiple scatter region.

In Tatarski's 1970 book [E3], which is a revised edition of his 1961 book [E2], he uses an alternative approach, which allows him to consider fluctuations in the multiple-scatter region when $\bar{\lambda}/\ell_m \ll 1$. (Here $\bar{\lambda}$ is the mean radiation wavelength and ℓ_m is the minimum correlation length associated with the index-of-refraction field.) He also now formulates the statistical problem in terms of the coherence function used in this report, instead of using phase and amplitude correlation functions. He presents a number of solutions for the coherence function in terms of the statistical properties of the index-of-refraction field. All his work is for isotropic fields, but when $\bar{\lambda}/l_m \ll 1$, it is not difficult to extend his work to include anisotropic fields. Both plane wave and finite-source solutions are given.

To the knowledge of the authors, the anisotropic medium problem has not yet been treated in the Soviet literature for the case when $\bar{\lambda}/\ell_{VM} = O(1)$. Soviet authors are, however, continuing to study the propagation problem from both an acoustic and an electromagnetic point of view.

In the Western literature there were a number of basic papers written for the single scatter region in the 1940's and early 1950's. Some of the contributors were Bergmann [E4], Pekeris [E5], and Mintzer [E6-E8]. G. Keller [E9] treated the mutual coherence function and obtained a correct expression for the multiple scatter region. Hufnagel and Stanley [E10] obtained a similar expression. Both these solutions contained unnecessary assumptions, but later work by Beran [E11] and Brown [E12] showed the conditions

under which the solutions were correct. Beran [E13] subsequently derived the basic governing equation that allowed the determination of the mutual coherence function for radiation propagating from a finite source when $\bar{\lambda}/\ell_m \ll 1$. This is the same result obtained by Tatarski [E3] using an alternative method. Also, as in the Soviet literature, solutions of this basic equation were obtained by a number of investigators. In all cases the solutions were for isotropic random media, but it is simple to extend the analyses to the nonisotropic case when $\bar{\lambda}/\ell_m \ll 1$. We found no solutions for anisotropic media in the multiple scatter region.

The literature of wave propagation in random media is vast and spread throughout a multitude of journals. In this very brief survey we were able to pass over this extensive literature by considering only those papers that are most germane to the objectives of the present study; i.e., obtaining multiple scatter solutions for the second-order coherence function in a problem in which the scattering is principally a forward scattering. We also note the neglect of papers concerned mainly with the mathematical aspects of obtaining formalisms on the moments of the inverse of a linear stochastic operator even though such formalisms are applicable to the scattering problem. The Bethe-Salpeter formalism, which can serve as a starting point for a derivation of Eq. (B11), is one result of this literature. Frisch [E14] presents a survey of the mathematical aspects of propagation in random media. This survey concentrates on the first two statistical moments of the radiation field.

REFERENCES

- E1. L. Chernov, *Wave Propagation in a Random Medium*, McGraw-Hill, New York, 1960.
- E2. V. Tatarski, *Wave Propagation in a Turbulent Medium*, McGraw-Hill, New York, 1961.
- E3. V. I. Tatarski, *The Effects of the Turbulent Atmosphere on Wave Propagation*, 1971; U.S. Department of Commerce, National Technical Information Service, Springfield, Va., 1970.
- E4. P. G. Bergmann, *Phys. Rev.* **70**, 486 (1946).
- E5. C. L. Pekeris, *Phys. Rev.* **71**, 268 (1947).
- E6. D. Mintzer, *J. Acoust. Soc. Amer.* **25**, 922 (1953).
- E7. D. Mintzer, *J. Acoust. Soc. Amer.* **25**, 1107 (1953).
- E8. D. Mintzer, *J. Acoust. Soc. Amer.* **26**, 186 (1954).
- E9. G. Keller, *Astron. J.* **58**, 113 (1953).
- E10. R. E. Hufnagel and N. R. Stanley, *J. Opt. Soc. Amer.* **54**, 56 (1964).
- E11. M. J. Beran, *J. Opt. Soc. Amer.* **56**, 1475 (1966).

- E12. W. P. Brown, IEEE Trans. AP-15, 1475 (1967).
- E13. M. J. Beran, J. Opt. Soc. Amer. **60**, 518 (1970).
- E14. U. Frisch, Ch. II in *Probabilistic Methods in Applied Mathematics* (A. T. Bharucha-Reid, editor), Academic Press, New York, 1968.

